2-D Seismic Reflection Interpretation of Line 2001-SNJ-02 (SP: 760-1099) of Sinjhoro Area (Southern Indus Basin) & Rock Physics Analysis

QUAID-I-AZAM UNIVERSITY
ISLAMABAD

Submitted By:

SHAFQAT HUSSAIN

(2008-2010)

Supervised By:

SHAHID IQBAL

A thesis submitted to the Department of Earth Sciences in partial fulfillment of the requirement of the degree of Master in Earth Sciences.

Department of Earth Sciences

Quaid-i-Azam University Islamabad

IN THE NAME OF ALLAH, THE MOST BENIFICENT AND THE MOST MERCIFUL

CERTIFICATE OF APPROVAL

This Thesis of **SHAFQAT HUSSAIN** is accepted in its present form by the Department of Earth Sciences as satisfying the requirement for M.Sc degree in **Geophysics.**

RECOMMENDED BY

DR. GULRAIZ AKHTER

(Officiating Chairman Dept. of Earth Sciences)

SIR SHAHID IQBAL

March 18, 2011

(Supervisor)

EXTERNAL EXAMINAR

DEPARTMENT OF EARTH SCIENCES

QUAID-I-AZAM UNIVERSITY

ISLAMABAD

DEDICATION

My whole thesis work is dedicated to my
Late Father.

ACKNOWLEDGEMENTS

ABSTRACT

Seismic line, 2001-SNJ-02 (SP: 760-1100) of Southern Indus Basin, was provided by the Department of Earth Science, Q.A.U Islamabad for interpretation. To investigate the lateral and vertical variation in the velocity, average velocity and Iso velocity map was generated.

A time section was produced from the seismic section using the shot points and the two-way-times (TWT) of the reflectors and faults. These average velocities were then used to find the depths of the formations for the Geoseismic Section or Depth Section.

For the interpretation of seismic data five reflectors are marked on the seismic section and named on the basis of nearby wells (Chak 63-01) in Southern Indus Basin which are Reflector 1 (Possible Laki Formation), Reflector 2 (Possible Ranikot Formation), Reflector 3 (Possible Khadro Formation), Reflector 4 (Possible Basal Sand) and Reflector 5(Possible Chiltan Limestone). Interpretation results indicate normal faulting in the Southern Indus Basin.

Different physical properties of the rocks are calculated and establish their relationship with depth. Reflection coefficients are calculated on different shot points and with the help of reflection coefficients lithologies are marked.

CONTENTS

Chapter No. 4   43-72

INTERPRETATION

List of Figures

Tables

APPENDICES

CONTENTS

CHAPTER # 01

INTRODUCTION

CHAPTER 01

INTRODUCTION

1.1 Introduction:

The study area forms a part of Southern Indus Basin that lies in southern part of Pakistan. The main tectonic events that control the structure forms in that region are related with the rifting of Indian Plate from Gondwanaland land (Jurassic to Early Paleocene).Rocks ranging in age from the Triassic to Recent occur in different parts of the area. Majority of the structures present are the normal faults because of the fact that it is related to rifting which caused normal faulting. The Southern Indus Basin is identified as an extension basin resulting from an inferred fossil-rift crustal feature overlain by a thick sedimentary sequence. Extension was a consequence of temporal divergence of the Indo-Pakistan subcontinent from Gondwanaland during the early Paleocene (Zaigham; 2000).

In the present dissertation, 2D seismic reflection data of line 2001-SNJ-02 (Sinjhoro area) is interpreted in order to view the subsurface geological aspects and hydrocarbon potential.

1.2 Objectives:

The present study is an attempt to explore the subsurface geology of part of Sinjhoro area of Southern Indus Basin. 2-D seismic reflection data of line 2001-SNJ-02 (S.P:760-1100) has been used to identify the prominent stratigraphic horizons and understand the tectonics and structural trends of the area and delineate the subsurface target horizons in the study area. Various parameters of the seismic line (average velocity, mean velocity and Iso-velocity graph etc.) have been used to investigate the lateral and vertical geologic variation in the area.

1.3 Methodology:

Sinjhoro is located in southern part of Pakistan, about 22.5 km northwest of Sanghar district of Sindh, and forms a part of Sindh Monocline. The given 2D-seismic reflection data was acquired and processed by Oil & Gas Development Corporation Ltd. (OGDCL) Pakistan.

In the present case, mean velocity and iso velocity graphs were prepared from the concerned velocity functions given on the seismic sections (Figs. 4.4 & 4.5 respectively). Then horizons of interest and faults, if present, were marked. Based on the marked horizons and above mentioned velocity functions, time section (Fig. 4.6) was prepared. Based on this time section a section in depth mode was prepared (Fig. 4.7) using the concerned velocity and other information. The depths information obtained for the marked horizons on depth section were then correlated (Table 4.1) with the well tops (well Chak 63-01) of the area and the horizons were then tentatively named. The same was then applied to the time section. Using tops of the identified horizons on time and depth sections as basis, time and depth contour maps (Figs. 4.8 & 4.10 respectively) were prepared for the horizons of interest. The faults were then also marked on these contour maps. This subsurface information was used to create a tentative model for trapping mechanism in the area.

1.4 Location, Accessibility and Base Map:

Sinjhoro is a small town in Sanghar District, along Sanghar-Shahdad Pur Road. It is bounded by Lat: $26°02'$ to $26°20'$ North and Long: $68°48'$ to $69°6'$ East (Fig. 1.1).

It is located in plain areas of Sindh province and is easily accessible by means of roads as well as trains. A base map showing boundaries and orientation of the seismic lines is shown in figure 1.2. From the base map, it is clear that most of the seismic lines are dip lines with some strike lines
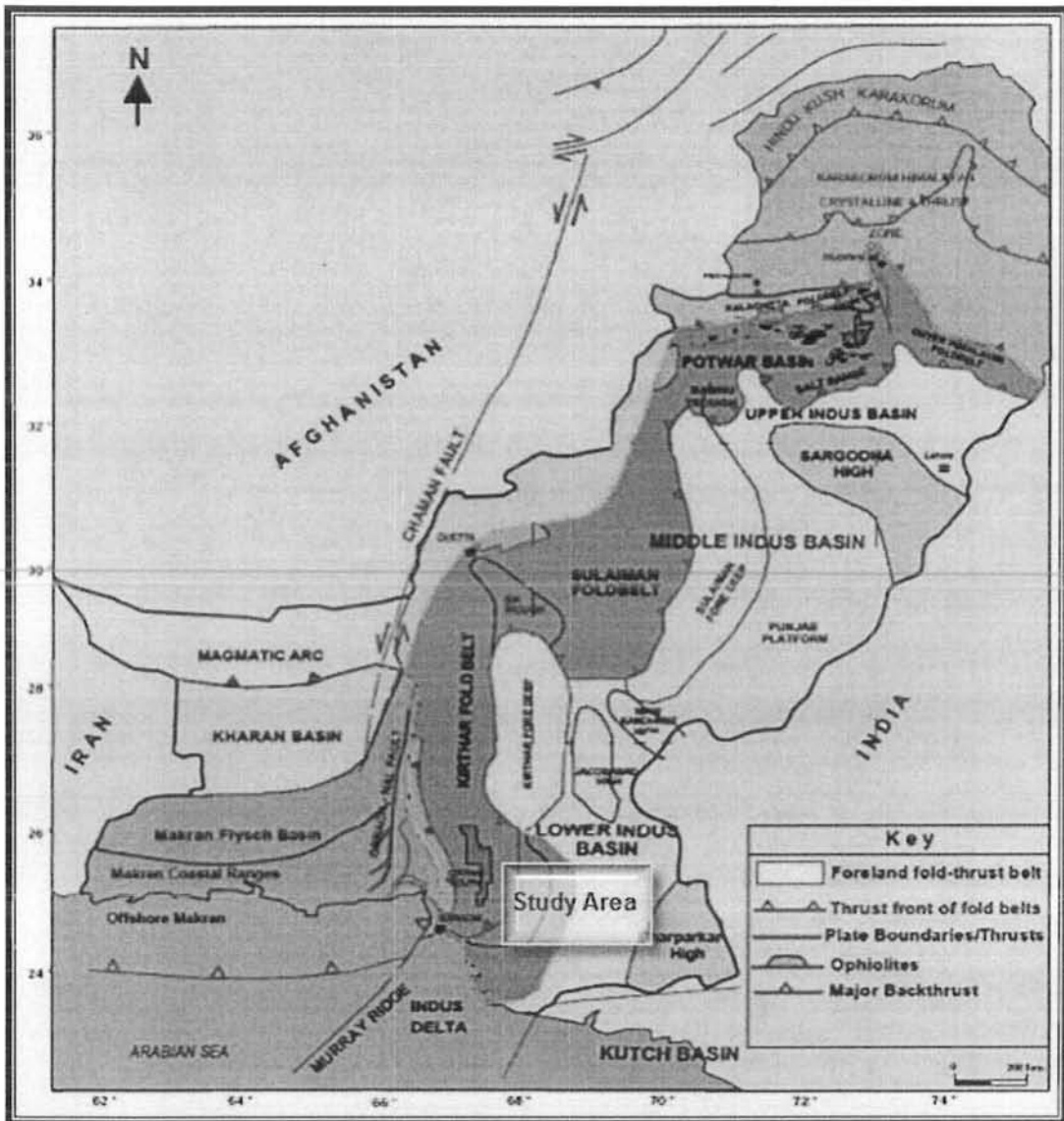
Figure 1.1 Location of Study Area in Pakistan (Kazmi and Snee; 1989)
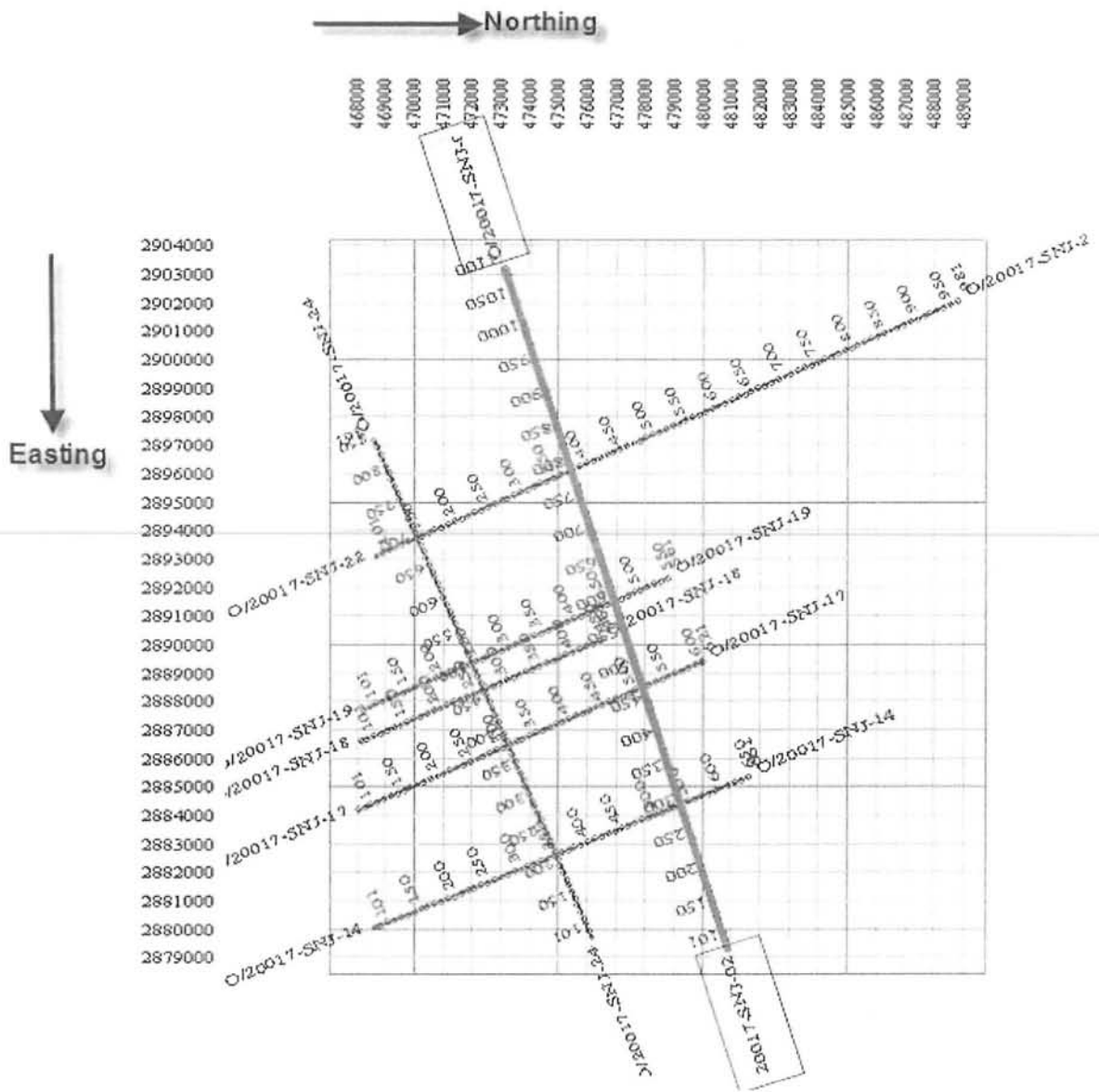
Figure 1.2 Base Map showing the Orientation of Line SNJ-02 (shown purple)

(2001-SNJ-02 & 2001-SNJ-24). The present dissertation is based on the strike line 2001-SNJ-02.

1.5 Previous Work:

Exploration in the Southern Indus Basin starts from 1939, when Burmah Oil Company drilled a 511m (1,676-ft) well near Karachi, called Drigh Road GIB 1. Prior to this well, several geologic studies had been conducted. Most of the previous work was of an academic nature, and had been undertaken by the Geological Survey of India. Burmah Oil Company drilled a 3,861-m (12,667-ft) well on the Lakhra structure in May 1948, and from 1955 onward, exploration for oil and gas accelerated in the Southern Indus Basin. All seismic surveys were single-fold. The first comprehensive geologic report was published in 1961 under the Colombo Plan Project (Hunting Survey Corporation, 1961) and contains geologic maps on a 1:250,000 scale. Landsat images were interpreted by the Technical Services Department now Offshore Department) of OGDC in collaboration with Hunting Geology and Geophysics Ltd., (Hunting, 1980). This survey delineated several lineaments and circular features in the area, which were important from a hydrocarbon exploration viewpoint. Currently, geologic surveys are being conducted on these features, and studies of the present Indus delta are envisaged in the near future (Qadri and Shuaib; 1986).

1.6 Topography & Climate:

The most area of the district is fertile plain formed by the canal except eastern desert area from Jamrao Head to Khipro Taluka. The soil is sandy with hard clay loams and some part is desert. The average elevation is about 50 meters above sea level.

Sanghar district has extremely hot climate. However, there is slight variation between the climate of north and western parts of the district. The south

western portion enjoys the advantage of sea breeze. The summer season commences from April and continues till October. May, June and July are the hottest months. The mean maximum and minimum temperature during this period is 42 and 25 degree centigrade respectively. The months of August and September are stuffy and suffocating. December, January and February are the coldest months. The mean maximum and minimum temperatures for these months are 25 degree centigrade and 8 degree centigrade respectively. The bright sunshine makes the district, in winter, one of the healthiest parts of the region.

1.7 Display Parameters of Seismic Line:

The seismic traces may be displayed in a variety of ways. Below mentioned are some of the techniques and their short description:

Scaling:

The seismic data plotting software will usually read in a default number of traces (e.g. 500) and determine the average amplitude. The rest of the plot will be scaled relative to this amplitude such that the display is visible.

Bias:

The bias can be used to alter the zero-amplitude baseline. An addition of bias (as a percentage of trace spacing) reduces the amount of black infill, making the display greyer in appearance. Some of the display parameters of the given seismic line (SNJ-02) are shown below:

(1)　Polarity: Normal

(2)　Traces per Inches: 36

(3)　Inches/Sec: 2.5

(4)　Bias: 0.0

CHAPTER # 02

GENERAL GEOLOGY

Chapter 02

GENERAL GEOLOGY

This chapter deals with the brief description about the tectonic settings, structural geology and stratigraphy of the study area. Petroleum significance of the area is also taken into consideration. Seismic data interpretation is based on the stratigraphy and structure geology of the area; therefore, it is important to have information about the geologic aspects of the area. The observations made in the present study have also been incorporated in the chapter.

The study area lies in the Southern Indus Basin so only the development of Southern Indus Basin will be discussed here.

2.1 Tectonic Setting:

The Lower (Southern) Indus Basin is bounded to the north by Sukkur Rift zone, to the south by Indus Offshore and the Kirthar Foredeep in the west and by Indian shield to the east as indicated in figure 2.1. Southern Indus Basin extends approximately between Lat. 24° to 28° N and from Long 66°E to eastern boundary of Pakistan.

The main tectonic events which have controlled the structures and sedimentalogy of the Southern Indus Basin are rifting of Indian Plate from Gondwanaland (Jurassic to Early Paleocene) which probably created NE-SW to N-S rift systems, isostatic uplift or ridge push at the margins of newly developed ocean probably caused uplift and eastward tilting at the start of the Cretaceous. Separation of Madagascan and Indian plates, in the Mid-Late Cretaceous, may have caused some sinistral strike slip faulting in the region, hotspot activity and thermal doming at the Cretaceous-Tertiary boundary. This in turn caused uplift, erosion, extrusion of the Deccan flood basalts and probably the NNW

North	Sukkur Rift Zone
South	Indus Offshore
East	Indian Shield
West	Kirthar Foredeep

Figure 2.1 Geological Boundaries of Southern Indus Basin
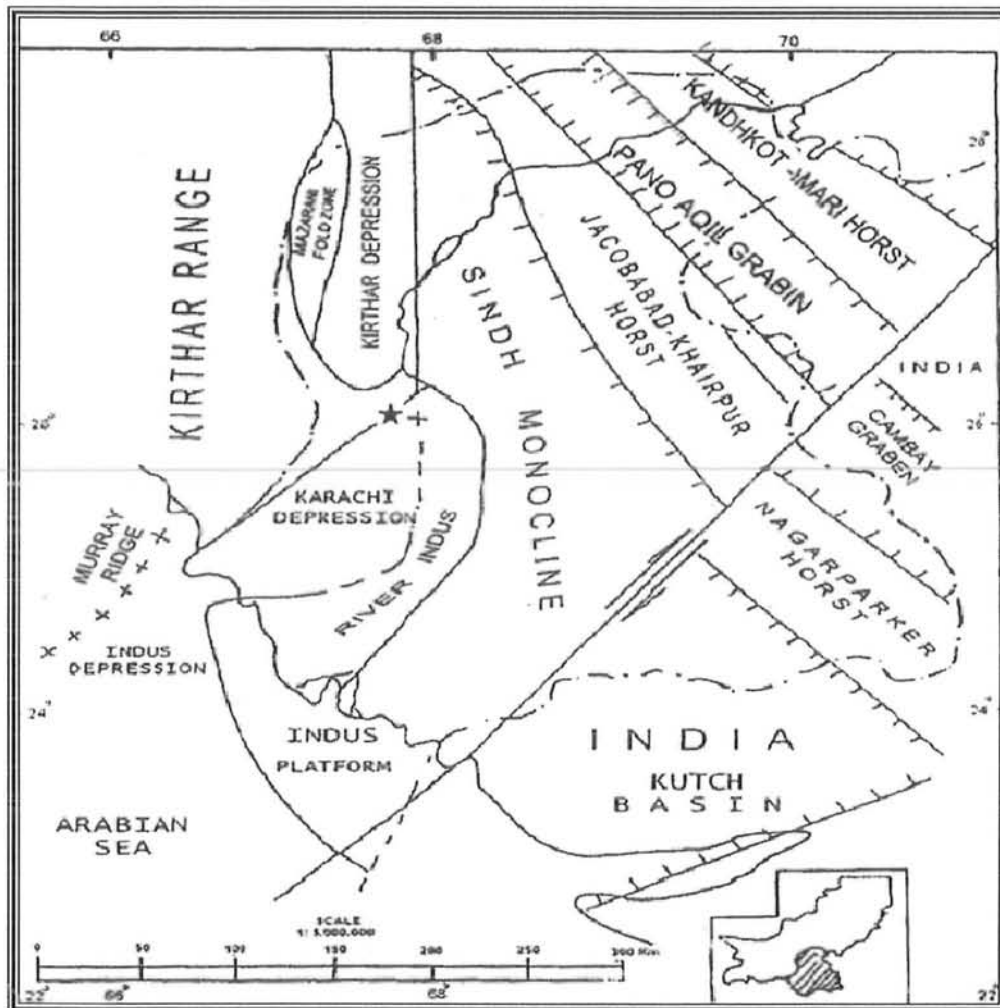
Figure 2.2 Tectonic Map of Sinjhoro Area showing Geological Boundaries (Kadri; 1995).

8

striking normal faults. Paleocene-Eocene emplacement of Bela Ophiolites may have caused gentle folding. Eocene passive margin conditions caused structural quiescence and carbonate deposition, Oligocene to present day. Himalayan collision caused sinistral transpression in the west of Lower Indus Basin, with fold-thrust structures overprinted by sinistral flower structures (Pakistan Petroleum Information Service, Report; Lower Indus Platform Basin).

2.2 Structures:

It is characterized by several structural highs. The study area, as previously mentioned is located in Southern Indus Basin and is characterized by a series of horst and graben present almost below the base. The seismic profiles of this region indicate gently dipping structures with abundant normal faults (Kazmi & Jan; 1997). Most of the basement faults are apparently Late Cretaceous and affect Mesozoic and earlier rocks. These Late Cretaceous faults mostly are rift structures. In Sindh, they are largely concealed beneath the Deccan Trap basalts and younger sedimentary rocks, so, unlike Central and Upper Indus Basins which are mostly comprised of reverse faulting structures indicating the collision, Lower Indus Basin has normal faulting structures in abundance indicating the effect of rifting more than that of collision among the plates i.e. indicating extensional regime. Some basaltic lava flows are also present as observed in Khadro Formation.

Zaigham and Mallick, 2000, proposed a structural model for the evolution of Southern Indus basin.

1. This corresponds to the initial rifting of the super continent Gondwanaland, probably during the Paleozoic (Smith & Hallam; 1970, Powell; 1979). The divergent phenomena includes the formation of Basaltic magma in the upper part of the asthenoshpere, causing broad tectonic up warp and thinning of the overlying Lithosphere, probably resulting from plastic flow in the lower part and extensional faulting in the upper part. The thinning of Lithosphere continued and resulted in the collapse of the tectonic up warp over the magma blister and

subsequently the process of sea floor spreading began with basaltic magma upwelling to the earth surface at oceanic Lithosphere.

2. Extensional forces broke the upper brittle crust into blocks separated by active faults during sea floor spreading. It appears that stretching of initial rifted part stopped at some geological time during very late Paleozoic to very early Mesozoic (Ahmed & Zaigham; 1993). The stretched crust remained as Indus basin failed rift in sediments started to accumulate.

3. The third step represents subsidence of the continental crust and simultaneous accumulation of the Mesozoic and Tertiary sediments in the Indus basin.

4. Thick Cenozoic strata are exposed along the western margin of the Indus basin in the Kirthar Fold and Thrust Belt.

5. Tertiary strata have also been reported from Jaisalmir and Ran Ketch areas. Unconsolidated quaternary sediments rang between 30m and 200m thick in the southern Indus basin.

Sindh Monocline:

Sinjhoro is a part of Sindh monocline which lies in lower Indus basin and situated at the Indo-Pakistan plate. It is triangular shaped with gentle slope. It is bounded in east by the Indian shield and merges into Kirthar and Karachi troughs in the west. In the north it is bounded by Sukkur rift zone. The Indus Offshore platform in the south is the extension of Sindh monocline (Fig. 2.2)

2.3 Stratigraphy:

The Southern Indus Basin acquired its stratigraphic features from tectonic events associated with plate movements. A generalized stratigraphic column of

10

Lower Indus Basin is shown in table 2.1. This column shows distribution, age and lithology of the area.

Triassic:

In the Triassic, shelf-system strata (of Upper Indus Basin) extended to the Lower Indus Basin and are preserved in the Triassic Wulgai Formation and Jurassic Shirinab Group. A carbonate-dominated shelf environment persisted at least intermittently on the western part of the Indian plate through Late Jurassic, exemplified by the interbedded shales and thick limestones of the Springwar Formation and as much as 1,400 m of the Middle and Late Jurassic Sulaiman Limestone Group, which accumulated on the western and northern portions of the Plate. Jurassic or earlier extensional tectonics and failed rifting along the Indus River contributed to a postulated deep-seated shear zone and horst-and-graben regime and later, a division of the greater Indus Basin into three subbasins at the Mari-Kandhot and Sargodha structural highs (Kemal, 1992; Zaigham and Mallick, 2000). Late Jurassic rifting also initiated separation of Australia and Antarctica from India (C.J. Wandrey, et al, USGS Bulletin 2208-C,"Petroleum Systems and related Geological Studies in South Asia").

Wulgai Formation:

The oldest rocks exposed/encountered in the area are of Triassic Wulgai Formation. The name Wulgai formation was used by Williams (1959), after the village of Wulgai near Muslimbagh.

The Formation is composed of dark grey to black and greenish clayey shale and mudstone with subordinate limestone in the lower part. In the middle inter-bedded shale, limestone, and sandstone is present. The limestone is dark grey to black, fine to medium grained and includes some sandy limestone beds. The mudstone and shale are dark grey, nodular, laminated and sandy with

ERA	PERIOD	EPOCH		FORMATION	LITHOLOGY	DESCRIPTION
CAINOZOIC	QUATER-NARY	RECENT		ALLUVIUM		SANDSTONE, CLAY SHALE AND CONGLOMERATE
		PLIO-PLEISTOCENE		SIWALIK		SANDSTONE, SHALE AND CONGLOMERATE
	TERTIARY	MIOCENE		GAJ		SHALE, SANDSTONE AND LIMESTONE
		OLIGOCENE		NARI		SHALE, LIMESTONE AND SANDSTONE
		EOCENE	LATE			
			MIDDLE	KIRTHAR		LIMESTONE AND SHALE /LAKI LIMESTONE AND SHALE
			EARLY	LAKI/GHAZIJ		GHAZIJ SHALE AND SANDSTONE
		PALEOCENE		BARA-LAKHRA		LIMESTONE, SHALE AND SANDSTONE
				KHADRO		BASALT AND SHALE
MESOZOIC	CRETACEOUS	LATE		PAB		SANDSTONE AND SHALE
				MUGHAL KOT		LIMESTONE, SHALE AND MINOR SAND
				PARH		LIMESTONE
		MIDDLE	GORU	UPPER GORU		MAIN SEAL SHALE AND MARL
				LOWER GORU		SHALE AND SANDSTONE MAIN SOURCE
		EARLY		SEMBAR		SHALE AND SANDSTONE
	JURASSIC	LATE				CHILTAN LIMESTONE
		MIDDLE		MAZAR DRIK CHILTAN		MAZAR DRIK LIMESTONE AND SHALE
		EARLY		SHIRINAB		LIMESTONE, SHALE AND SANDSTONE
	TRIASSIC	EARLY-LATE		WULGAI		SHALE AND SANDSTONE

LEGEND
- ● OIL
- ☼ GAS
- Sst
- Clay
- Lst
- Sh
- Cong
- Basalt

Table 2.1 Generalized Stratigraphy of Southern Indus Basin

(Modified from Raza ET AL, 1990)

carbonaceous inclusions. The upper part is composed of shale, marl and limestone of black, dark grey and greenish-grey color. The limestone is crystalline. The marly beds contain ammonites.

In the Wulgai section, the Formation though disturbed, is estimated to be 1,180 m thick (Williams; 1959). According to Sokolov and Shah (1965) the total thickness of Triassic sediments is 985m.

The upper contact with the Jurassic rocks is transitional. The lower contact with the Permian beds is tectonically disturbed in the Wulgai section, disconformable in the Ghazaband section, but conformable in the Shirinab section (Hunting Survey Corporation; 1961; Sokolov and Shah; 1965).

The presence of ammonites such as *Halorites, Jovites, Pararcestes, Arietocelites,* and the bivalve *Halobia* in the upper part and of *Columbites* in the lower part, indicate an Early to Late Triassic age.

The Formation may be correlated with the Mianwali, Tredian, and Kingriali Formations of the Salt Range and Trans-Indus ranges. It is correlated with the lower parts of the Shirinab and Zidi Formations and represents almost all of the Alozai Group and lower part of the Tindar Group of Hunting Survey Corporation1961.

Shirinab Formation:

The name Shirinab was introduced by Hunting Survey Corporation (1961) for undifferentiated Jurassic, Triassic and even Permian rocks. It is derived from the name of the river that drains the Chappar, Mingochar and Shirinab valleys.

In the type area, the Formation consists of interbedded limestone and shale which grades downward into a dominant shale lithology (Wulgai Formation) of Triassic age and is either overlain transitionally by the Chiltan limestone or disconformably by the Sembar and Goru formations or younger rocks? The

limestone is thin to medium-bedded, grey to dark gery and black. ; It is finely crystalline to fairly coarse-textured with shely, oolitic, pellitic and pisolilic interbeds. The lower part locally includes sandstone intercalations; associated shale is of grey to dark grey our but occasionally orange-yellow, green and varieties are also present. The shale is calcareous and ranges from soft flaky to hard fissile platy.

Away from the type locality, the Formation may be divided into three members depending on the increase or decrease of shale in the generally thin to medium-bedded limestone.

The three members of that formation are the following.

(a) Anjira member

(b) Loralai limestone member

(c) Spingwar member

(a)Spingwar member:

Consists of interbedded dark grey to black limestone and calcareous shale. The limestone is finely crystalline, but in some areas oolitic, pellitic and shelly beds occur in the upper part, while sandstone interbeds are present in the lower part.

The member is 648 m thick in the type section at Spingwar (designated by Williams) north of Zamari Tangi, about 35 km northwest of Loralai. The member thickens to approximately 1818 m near Gormai in the Loralai District. Williams (1959) and Woodward (1959) have reported a wide distribution of the member in the Sulaiman-Kirthar provinces and the Axial Belt. The Spingwar member has yielded Early Jurassic fossils, including ammonites. It is underlain transitionally by the Wulgai Formation of Triassic age and is overlain (in the Khuzdar and Loralai areas) by the Loralai limestone member.

(b) Loralai limestone member:

Distinguished from the underlying Spingwar member by the predominance of thin to medium-bedded grey, dark grey and black limestone. Shale is very subordinate and is present as thin partings at different levels. The limestone is generally fine grained, but oolitic, pisolitic and pelleted beds are reported from the upper part.

The member is widely developed in the Loralai district where it forms prominent hills. In the type area designated by Williams, Zamari Tangi in Loralai District, the thickness is 424m but further north, according to Woodward (1959), it diminishes to 6 m and from many parts of Lower Indus Basin the member has not been distinguished from other parts of Shirinab formation.

The age assigned by Williams and Woodward is Early Jurassic, but Hunting Survey Corporation has recorded Toarcian fossils from fairly low levels in the Loralai limestone. According to them, the upper part may represent the rest of the Jurassic. In parts of Loralai area the member is overlain disconformably by the Sembar formation while in Khuzdar area it is transitionally overlain by Anjira member.

(c) Anjira member:

Type section designated by Williams, 1959, 12 km east of Anjira village in the western Kirthar Range) is recognized as a distinct unit in the western Kirthar Range, south of Kalat and in the Axial Belt area around Khuzdar. The rocks included in the Anjira member are dark grey, thinly bedded limestone, softer argillaceous limestone and calcareous shale. The limestone is generally fine textured; sub lithographic the type area the thickness is 90 m but in Khuzdar, it thickens 367m to 312m is recorded from Sundhi Nala (Woodward, 1959). The member is overlain disconformably by the Sembar or Goru formations of Early Cretaceous age. The age assigned by Williams (1959) and Woodward (1959) is Toarcian to early Bajocian.

The Formation is widely developed in the Sulaiman and Kirthar provinces and more particularly in the adjoining Axial Belt. The Shirinab formation in its type area is estimated to be between 1,515 m and 3,030 m thick. Fossils recorded from different parts of Sulaiman-Kirthar provinces and Axial Belt indicates an Early Jurassic age, but the upper part may extend into the Middle Jurassic.

The rock unit may be correlated with Shainawarai Formation and other rocks in the adjoining areas of Madagascar and Saudi Arabia and also with the similar rocks in Iran.

Jurassic

Chiltan Limestone:

The name Chiltan Limestone was introduced by Hunting Survey Corporation (1961) and is derived from the Chiltan Ranges Southwest of Quetta.

The Chiltan limestone is composed of massive, thick bedded, dark limestone, but shows colour and texture variations within one section and in different areas. The colour varies from black, dark grey, grey, light grey, brownish grey, bluish grey to occasionally white. Pisolitic limestone beds are present locally. The texture varies from fine-grained, sub-lithographic to oolitic, reefoid and shelly. Veins and nodules of black or rusty weathering chert are present locally.

Williams (1959) gave a thickness of 757m in Dara Manda Nala which is 3 km south of Bostan. Hunting Survey Corporation estimated a thickness of 1,818 m in the region of Quetta and Dhanasar.

The Chiltan limestone has not yielded identifiable fossils though poorly preserved fragmentary remains are found occasionally. Its stratigraphic position above the Shirinab formation or its Loralai limestone member of Early Jurassic

age and below the Mazar Drik formation (" Polyphemus beds") of Early Callovian to Late Bathonian suggest the age to be mainly Middle Jurassic.

The formation where developed, overlies the Shirinab formation or its Loralai limestone member with a gradational contact that is spread over an interval of 15 to 30 m and is marked by a change of thick-bedded limestone to thin-bedded limestone and intercalated shale of the underlying Shirinab formation. The upper contact with the Mazar Drik formation (" Polyphemus beds " of Vredenberg) is gradational but in many areas this upper limestone is not developed and recognized and the Chiltan limestone has a disconformable contact directly with the overlying Sembar formation of mainly Early Cretaceous age.

The Chiltan Limestone correlates with the Samana Suk Formation of the Upper Indus Basin, but shows significant lithological changes in having darker, thicker and more massively bedded limestone, with hardly any shale and marl intercalations.

Cretaceous:

During Early Cretaceous time the Indian plate drifted northward, entering warmer latitudes. On the western shelf, marine shales, limestones, and near shore sandstones of the Lower Cretaceous Sembar and Goru Formations were deposited over a regional erosion surface on the Sulaiman Limestone Group. In the Kohat-Potwar area, this erosion surface is present at the top of the Samana Suk Limestone Formation and is overlain by Lower Cretaceous Chichali Formation sandstones and shales (Shah, 1977; Iqbal and Shah, 1980). Along the eastern portion of the Indian plate, Rajmohal Trap volcanics and the Bolpur and Ghatal Formations were deposited. Although the carbonates are recognized primarily on the eastern and western shelves today, it is likely that they were deposited over much of the northern Indian shelf. This shelf environment persisted through Late Cretaceous time when regressive sandstones such as the

17

Lumshiwal and Pab Formations in the west and Tura Formations in the east were deposited.

During Late Cretaceous time the Indian plate continued drifting northward toward the Asian plate, the seafloor of the Bengal Basin began to form, and flysch accumulated around much of the Indian plate. Northward plate movement continued during the latest Cretaceous, and a transform fault became active along the ninety-east ridge. In the Assam area, a southeasterly dipping shelf and block faulting developed. Rifting between Madagascar and the Seychelles initiated formation of Mascarene Basin. Extensional faulting occurred or was reactivated as the western part of the Indian plate sheared southward relative to the main plate. Counter-clockwise rotation of the Indian plate was initiated, and the Seychelles portion of the Indian plate began to break away (Waples and Hegarty, 1999). Latest Cretaceous time also brought to western India intense volcanism, expulsion of the Deccan Trap basalts, and further rifting, which began, and then failed, leaving the Cambay and Kutch Grabens just south of the Lower Indus Basin floored with the Deccan Trap basalts (Biswas and Deshpande; 1983).

Sembar Formation:

The name Sembar Formation was introduced by Williams (1959), after Sembar Pass in the Marri hills. The type section of the formation is about two kilometres southeast of Sembar Pass in the Marri-Bugti area, Sulaiman Province.

The Sembar Formation consists of black silty shale with interbeds of black siltstone and nodular rusty weathering argillaceous limestone beds or concretions. Glauconite is commonly present which gives the greenish hue to the weathering colour. In the basal part pyritic and phosphatic nodules and sandy shales are developed locally.

The thickness in the type section is 133 m but the Formation thickens to 262 m in the Moghal Kot Section of the Sulaiman Range and has been reported

to be much thicker in the subsurface (Williams, 1959). In some areas such as the vicinity of Quetta and Ziarat, the thickness of the formation is reduced to a few metres and the formation is absent in parts of Axial Belt and the Kirthar Province where the overlying Goru formation directly overlies the Jurassic limestone.

Its lower contact with various Jurassic Formations such as Mazar Drik formation, Chiltan limestone and Shirinab formation is disconformable while the upper contact is generally gradational with the Goru formation.

The Formation is reported to contain foraminifers, but the most common fossils are the *belemnites Hibolithes pistilliformis, H.* siibfusiformis and *Duvalia* sp. The *Hibolithes* spp., though regarded as early Neocomian (Berriasian-Valanginian), may not be restricted to this age as comparable species from the Salt Range and Trans-Indus ranges have been found to be associated with Late Jurassic ammonites (Fatmi; 1968, 1972). The age of the formation, though mainly Neocomian, most likely extends into the Late Jurassic. The Sembar Formation is correlated with Chichali Formation of the Kohat-Potwar Province.

Goru Formation:

The name Goru Formation was introduced by Williams (1959). The type section is situated near Goru Village on the Nar River in Southern Kirthar Range.

The Formation consists of interbedded limestone, shale and siltstone. The limestone is fine grained, thin bedded, light to medium grey and olive grey in colour. The interbedded shale and siltstone are grey, greenish grey and locally maroon in colour. The shale varies greatly in proportion and in places is the dominant rock type. Limestone is dominant in the lower and upper parts of the formation.

The Goru Formation is widely distributed in the Kirthar and Sulaiman provinces. It is 536 m thick in the type locality, but the thickness decreases to 60 m near Quetta.

The lower contact with the Sembar Formation is conformable, though locally an unconfirmity has been reported by Williams (1959). In some parts of the Axial Belt, for example, of Khuzdar, the Goru Formation directly the Jurassic limestone and the Sembar lithology is not developed. The contact between and Sembar formations is placed at the appearance of frequent limestone interbeds. The contact with the parh limestone is transitional and is placed at the last shale interbed.

The Formation contains foraminifers and belemnites (*Hibolithes* spp.).The age of the formation is assessed mainly as Early Cretaceous though the upper age limits in many areas extend into the Late Cretaceous and the lower age limit may extend down into the Late Jurassic. The Goru Formation may be correlated with the Lumshiwal Formation of the Kohat-Potwar Province.

Parh limestone:

The term "Parh" was introduced by Blanford (1879) for the rocks of Parh Range. Williams (1959) redefined it as a limestone formation between the Goru and Mughal Kot formations. The type area lies in the Parh Range in the upper reaches of the Gaj River.

The Parh limestone is a lithologically very distinct unit. It is a hard, light grey, white, cream, olive green, thin-to-medium-bedded, lithographic to porcellaneous, argillaceous occasionally platy to slabby limestone, with subordinate calcareous shale and marl intercalations. The porcellaneous nature and the concoidal fracture distinguish it from other limestone units. In the lower part an impersistent, maroon-coloured limestone bed is developed near the contact with the Goru formation.

The formation is widely distributed in parts of the Axial Belt and Lower Indus Basin. In the type area the thickness is 268 m but varies from 300 to 600 m in other areas.

The formation is rich in foraminifers (*Glnbotruncana* spp.) and is dated as Late Cretaceous. The foraminifers include *Globotruncana ventricosa*, *G. lapparenti*, *G. sigali* and *Pseudotextularia elegans* (*Gig on*, 1962).

The Formation is correlated with the Kawagarh Formation of the Kohat-Potwar Province.

Paleocene:

From Late Cretaceous through middle Paleocene time, trap deposits and basal sands continued to accumulate on the Assam-Arakan, Indus, Bombay, and Bengal shelves. Oblique convergence of the Indo-Pakistan plate with the Afghan and other microplates resulted in wrench faulting and development or reactivation of regional arches such as the Jacobabad and Sargodha Highs in the Indus Basin (U.S. Geological Survey Bulletin 2208-C).

Khadro Formation:

The name Khadro Formation was introduced by Williams (1959) and he designated Bara Nai in the northern Laki Range as the type section.

The formation consists of sandstone and shale, with some limestone. The sandstone is olive yellowish brown, grey and green, soft, medium-grained, ferruginous and calcareous. The shale is olive, pale bluish grey, chocolate and reddish brown and gypsiferous and contains thin interbeds of grey to brown argillaceous, in places arenaceous, limestone in the lower half of the unit. Both sandstone and limestone are fossiliferous. At the type locality the basal part of the unit consists of dark limestone bed with oysters and reptile bones. A number of basaltic flows (at least two) are present that are partly massive, partly amygdaloidal, brecciated and weather black. Top of the unit is usually marked by a volcanic flow. At Karkh and Jakker, the formation consists dominantly of interbedded soft, brown and olive shale and soft, grey to green, well bedded sandstone. The Karkh occurrence contains fragments of greenish and rusty

21

weathering vesicular rock and locally thin layers of dense, black basalt. Some marl beds are also present. Some conglomerate layers, consisting of pebbles and chips of red jasper, marl, limestone, red and green lava, diorite, black basalt and pink granite are present in Thar.

The Formation is widely distributed in the Kirthar Province and Calcareous Zone and parts of the Arenaceous Zone of the Axial Belt. The formation has only been reported from one locality (Rakhi Nala) in the Sulaiman Province where it is 170 m thick but there is a possibility of its being present in other parts of the province as well. It is 67 m thick in the type section, 140 m in the subsurface at Lakhra, and 180m in the subsurface at Dabbo Creek.

The Formation unconformably overlies the Moro Formation and Pab sandstone. It is apparently overlain conformably by the Bara Formation.

Eames (1952) reported *Corbula (Vancorbula) harpa, Leionucula rakhiensis, Venericardia vre-denbtirgi, Tibia (Tibiochilus) rakhiensis* and other fossils from the Rakhi Nala and assigned an Early Paleocene age to the unit. A long list of Foraminifera has been given by Hunting Survey Corporation (1961). Douville (1928) also described a fauna from the Formation, age of the Formation is regarded as Early Paleocene which, in places, extends into Late Cretaceous as indicated by the presence of *Globotruncana* (Hunting Survey oration; 1961).It may be correlated with lower part of the Rakhshani Formation in the eruptive Zone of the Axial Belt.

Ranikot Group:

In the Kirthar area of Lower Indus Basin, the Paleocene succession consists of the Ranikot group.The group is named after Ranikot Fort, in the northern part of Laki range, Sindh. It includes *Cardita beaumonti* beds, (Blanford;1879).

The group has a basal marine sequence of sandstone and shale with intrebeds of limestone and basaltic lava flows (Khadro formation), a middle fluviatileto paralic sequence of sandstone and shale with coal and carbonaceous beds (Bara Formation), overlain by marine limestone and some estuarine sandstone and shale (Lakhra Formation),followed by an upper sequence comprising grey, yellow to reddish brown sandstone siltstone and conglomerate (Sohnari Formation).

Eocene:

Laki Formation:

The term "Laki Series" was proposed by Noetling (1903).Later Hunting Survey Corporation (1961) redefined the unit as "Laki group".

In parts of the Kirthar Province, two distinct members are identified in the lower part of the formation. The basal member is named Sohnari member, after Sohnari, south of Meting (following Hunting Survey Corporation, 1961) which represents the " Basal Laki laterite" of Nuttall (1925). The Sohnari member, which overlies the Ranikot group, is itself overlain by the "Meting shales and limestone" of Vredenburg (1906) which are here formally named Meting limestone and shale member.

Mari Nai, southwest of Bara Nai, of the northern Laki Range, is designated as the type section of the formation. A section exposed about 5 km south-southwest of Meting is designated as the type section of the Sohnari member and meting limestone and shale member.

The Formation is composed of cream coloured to grey limestone but marl, calcareous shale, sandstone and lateritic clay may become significant constituents of the formation locally. In parts of the Kirthar Province, both the members are recognized in the lower part of the Formation.

The Sohnari member consists of vary coloured lateritic clay and shale with locally developed beds of yellow arenaceous limestone, pockets of limonite or ochre and lignite seams. Lenticular beds of variegated, ferruginous sandstone and white, calcareous sandstone are common in the member.

The Meting limestone and shale member consists mainly of creamy white nodular limestone in the lower part and interbedded shale and limestone with subordinate sandstone in the upper part. The shale is grey, greenish yellow, weathering dark rusty brown, ferruginous and gypsiferous. The limestone is thin bedded and arenaceous whereas the sandstone is commonly ferruginous.

The Formation is mainly developed in the Southern part of the Kirthar Province and in the vicinity of the Marri-Bugti hills in the Sulaiman Province.

It is about 240 m thick in the Bara Nai and the type locality (Mari Nai), but attains more than 600m thickness at Tatta (Kirthar Province) and Sui (Marri-Bugti hills). The *Sohnari member* varies in thickness from 1 to 15 m. The Meting member is 70 m thick at the type locality.

The Formation is unconformably underlain by the Ranikot group and the contact is marked by the *Sohnari member*. Its upper contact with the Kirthar formation in most areas of the Kirthar Province is conformable. In the northern parts of the Kirthar Province and throughout its development in the Marri-Bugti hills, the Formation is overlain by the Ghazij formation. In many localities of Lakhi Range, the Nari formation and the Siwalik group unconformably overlie it.

The Formation contains rich fossil assemblages including foraminifers, gastropods, bivalves, echinoids and algae, as reported by Noetling (1905), Nuttall (1925), Davies (1926), Haque and Khan *(in* Lexique, 1956), Haque (1962a), Hunting Survey Corporation (1961) and Iqbal (1973). The foraminifers include *Assilina granulosa, A. pustulosa, Lockhartia hunti* var. *pustulosa, Flosculina globosa, OpertorbitoUi.es douvillei, Fasciolites oblonga, Linderina brugesi* and *Dictyoconoides vredenburgi.* Important molluscs are *Gisortia*

24

murchisoni, Velates per-versus, and *Blagraveia sindensis.* Among the echinoids *Amblypygus subrotundus* and *Echino-lampas nummulitica* are common. These fossils indicate an Early Eocene age.

The Formation is correlated with the Kharan Formation and lower parts of the Saindak and Nisai Formations of the Baluchistan Basin, and parts of the Chharat Group of the Kohat-Potwar Province.

2.4 Petroleum Prospects:

Six proven and viable places are identified in the lower Indus basin, where perfect petroleum system exists.

Source Rocks

Early Cretaceous rocks are considered to be the potential source rocks for the hydrocarbon generation in the Lower Indus Platform Basin.

The lower Cretaceous shales of Sember Formation (as described above) are proven source for oil and gas discovered in the Lower Indus Basin because of its organic richness. The Lower part of the Goru Formation is moderately rich in organic shale having fair to good genetic potential amorphous organic matter rich oil prone karogen become dominant and can be regarded as "Potential source rock". Paralysis analysis results of Shahdad Pur well indicate that in Lower Goru Formation from 3225 m to bottom depth, there is a zone of maturity transition from oil and wet gas generation to dry gas generation (Kadri, 1995).

The source rocks of the Sembar (composed of shales) was deposited in shallow marine environments, are of mixed type-II and type-III karogen, with total organic carbon (TOC) content ranging from less than 0.5 percent to more than 3.5 percent; the average TOC of the Sembar is about 1.4 percent.

Thermal generation of hydrocarbons in the Sembar Formation began 65 to 40 million years ago, during Paleocene to Oligocene time. Hydrocarbon expulsion, migration, and entrapment are interpreted to have occurred mainly 50 to 15 MYA during Eocene to Miocene time, prior to and contemporaneously with the development of structural traps in Upper Cretaceous and Tertiary reservoirs (U.S. Geological Survey Bulletin 2208-C).

Reservoir Rocks

Cretaceous to Eocene clastics and carbonates are the proven reservoirs in the basin. Sands of Lower Goru (Cretaceous) Formation are the primary objective in this area. Average porosities for these sands are around 11% in the prospect area (Kadri; 1995).

Seal Rocks

A thick stratigraphic sequence of shale and marl of Upper Goru Formation serve as cap rock for underlying Lower Goru Sand Reservoir. Shale of Lower Goru Formation also has the same properties (Kadri; 1995).

Trapping Mechanism

Trapping mechanism in the southern Lower Indus Basin and in the Jacobabad-Mari-Kandkot High areas consists of the tilted fault blocks, faulted gentle role-over. Stratigraphic traps are also present.

CHAPTER # 03

DATA SETS

CHAPTER 03

DATA SETS

3.1 Introduction:

The present study is concerned with the 2D seismic interpretation of the Sinjhoro area in the Southern Indus Basin. The Seismic Line provided for this purpose is 2001-SNJ-02. On this seismic profile many prominent horizons may be observed, due to the acoustic impedance contrast, at different locations. In order to interpret the geology of Sinjhoro area using this line, various basic parameters were provided on the profile and some other important parameters were calculated from these already given parameters. Thus, the data sets for the time and depth sections were prepared, which were then used in the interpretation. In the following line a detail of these parameters and data sets is given:

3.2 Seismic Line Parameters:

On the seismic line different parameter related to acquisition, processing and display of the line were given. Amongst these important parameters some are mentioned below:

3.2a Display parameters:

Display parameters are the information related to the seismic section such as scale, time per inch/sec on it etc. Display parameters for the line SNJ-02 are given below:

Polarity: normal

Traces per inches: 14

Inches per sec: 3.75

Display amplitude: 10DB

Header contains information about the different parameters involved in acquisition and processing sequence which are given below.

3.2b Acquisition parameters:

The migrated, data was acquired in OCTOBER 2001. The line contains shot points from 104-1100. Some of the important recording parameters are given below.

Recording Parameters

Recorded By	:	OGDCL
Party number	:	SP-7
Data recorded	:	October 2001
Energy Source	:	Dynamite
Hole Depth	:	30m
No. Of Holes	:	01
Charge	:	03kg

Instrument

System	:	SN-358
Format	:	32-SEG D/DEMUL
Notch Filter	:	1N

Field Sampling Interval   :   2 MS

Record Length   :   5 SECONDS

No. Of Data Traces   :   240

Spread   : SYMMETRIC

CHANNEL

01	120	Shot	121	240

OFFSET

-3012.M	- 37.5 M	37.5 M

3012.5M

Station Interval   : 50 METERS

Group Interval   : 25 METERS

Type of Geophones   : SM-4 SERCEL/10 HZ

Geophones/Group   : 0212 OVER 23.92 M

Geophone Interval   : 1.04 M

3.2c Data Processing

After the data has been acquired, it passes through the whole processing sequence that includes different data processing techniques that are used to enhance the quality of the data.

This data has passed through a desirable processing sequence and finally a "Time Section" was prepared. The time section gives the position of different reflectors in terms of two way reflection times; therefore first we have to convert it in to time section to get the true picture of subsurface. Later on time section was converted in to depth section by estimation velocities so the processing sequence is given below.

Processing Sequences

Reformat to WGC CODE-4.

Resample 4 MSEC.

Geometry update.

Bad trace edit/reverse.

Uphole time statics update.

Geometrical Spreading Compensation.

Notch Filter 50 Hz.

CDP Sorting.

Zone Anomaly Process.

Surface Consistent Deconvolution.

Single Window.

Operation Length = 200MSec.

Whitening Noise = 0.1%

Prediction Distance =08 MSec.

Trace Balance After Decon.

Velocity Analysis.

Miser® (Surface Consistent Residual Statics).

Max. Statics Shift=20MSec.

Velocity Analysis.

Miser® (Surface Consistent Residual Statics).

Max. Statics Shift=24MSec.

Normal Moveout.

Start Time Mute.

Datum Reduction.

Stack.

Finite Difference Migration.

BP Filter.

Time (MSec)	Low cut (Hz)	High cut (Hz)
0-4000	10-14	40-45

19. Random Noise Attenuation

20. Time Variant Trace Equalization.

Length of First Zone   256MSec

Length of Longest Zone   512MSec

In Figure 3.1, a systematic diagram is given below explains the stages involved in data processing.

3.3 Processing

Data reduction is done by certain processing operations as discussed below.

- Demultiplexing
- Geometry definition
- Correlation
- Header generation
- Display
- Editing and muting
- Amplitude adjustment

3.3.1 Demultiplexing:

Data recorded on digital magnetic tape is not suitable for analysis therefore it is assembled from the digital tape by a sorting process. Thus "the process of sorting data from the magnetic tape into individual channel sequence is called Demultiplexing (Robinson & Coruh; 1988).

3.3.2 Correlation:

Correlation is simply the measurement of similarity or time alignment of two traces. Since correlation is a convolution without reversing the moving array, a similar frequency domain operation also applies to correlation. (Yilmaz; 2001). There are two types of correlation;

- Cross Correlation
- Auto Correlation
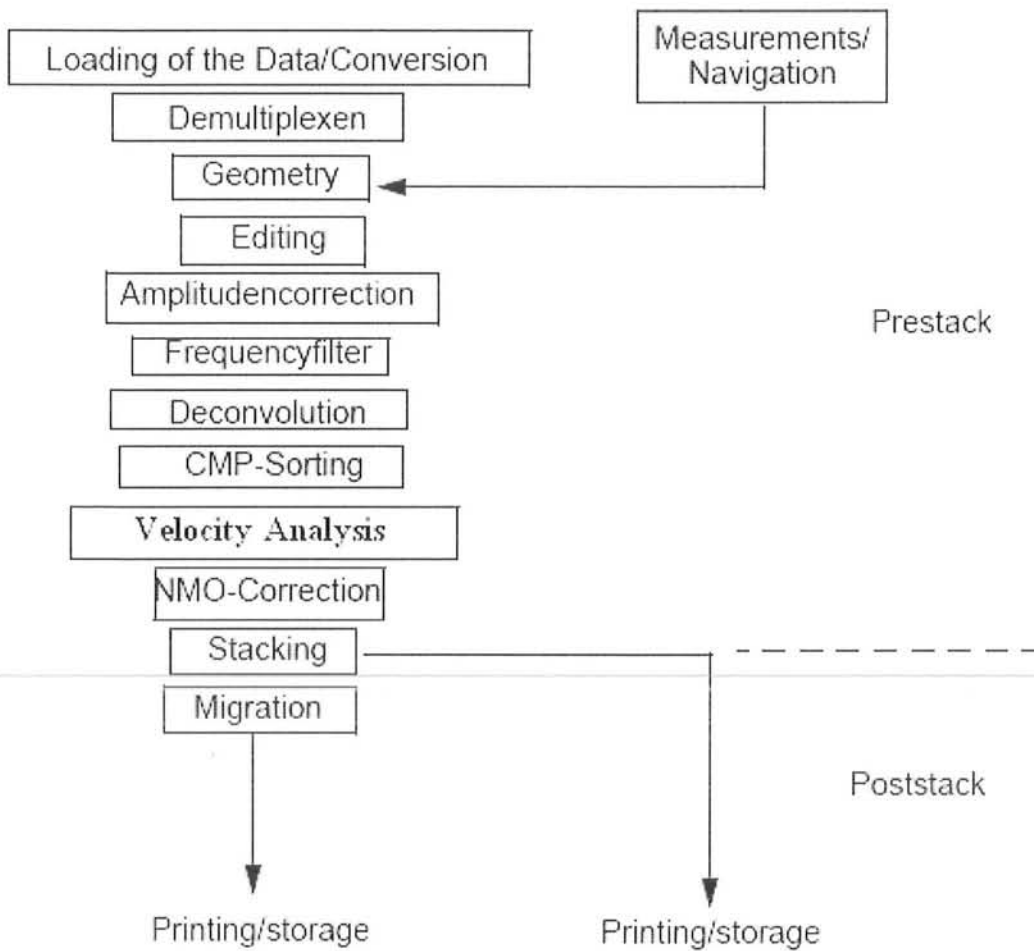
Figure 3.1 Block diagram showing the various stages of seismic processing
(Modified from Rehman; 1989)

(1) Cross Correlation

Cross correlation measures how much two time series resemble   each other. It is not commutative; output depends upon which array is fixed and which array is moved. As a measure of similarity, cross correlation is widely used at various stages of data processing (Yilmaz; 2001).

(2) Auto Correlation:

Correlation of a time series with itself is known as auto correlation. It is a symmetric function. Therefore only one side of the auto correlation needs to be computed (Yilmaz; 2001).

3.3.3 Header Generation:

After all of the sample from a given field trace are assembled into an array, a large amount of archival information is placed in a reserved block called a trace header, which is located on the just ahead of the data samples.

3.3.4 Editing and Muting:

Raw seismic data contains unwanted noise and sometime dead traces due to instrumental reasons. Thus the quality of data recorded is first observed by visual examination of raw field traces. Data may be affected by following reasons

- Polarity reversals in data
- Poor traces as well as poor bits

To remove polarity reversal, trace with reverse polarity is multiplied with it that becomes a trace with the polarity. Therefore editing is a process of removing or correcting traces, which in their original recorded taken, may cause stack deterioration (Rehman; 1989).

Each trace in one CDP is identified by it s shot point and receiver numbers. The CDP-gathers may be displayed as such for direct inspection and checking of edited data.

Muting

Trace-muting is a special type of data editing. This term is applied for process of zeroing the undesired part of a trace. In order to avoid stacking non-reflection events (such as first arrivals and refraction arrivals) with reflection, the first part of the trace is normally muted before carrying out the stacking process .This is occasionally referred to as first break suppression (Al.Sadi;1980).

3.3.5 Amplitude Adjustments:

Amplitude adjustment is done to recover the true information present in the data. Along with this effect, signal is further modified by recording station. So reflection amplitude recorded in the field is the end-result of the interaction of the following main factors;

- Spherical divergence
- Inelastic attenuation

3.4. Geometric Corrections:

In order to compensate for the geometric effects, we have to apply certain corrections on the recorded data .These corrections are called as geometric corrections (Dobrin & Savit; 1988). These corrections are applied on the traces gathered during trace editing and muting .The geometric corrections are

- Static correction
- Dynamic correction

3.4(a) Static Corrections

Static correction compensates the effect of weathered layer and elevation effect due to unleveled surface (Fig. 3.2).

Static correction is of two types:

(1). Elevation correction

(2). Weathering correction

3.4(b) Dynamic Corrections:

Dynamic correction compensates the effect of offset of receiver from the source. It is also related to the shape of the subsurface interfaces.

It is of two types:

a- Normal move out correction (NMO)

b- Dip move out correction (Robinson & Crouch; 1998)

3.5. Data Analysis and Parameter Optimization:

Three steps involved in this procedure. These three are:

Depth Model with Low-Velocity Layer

Depth Model After Static Corrections
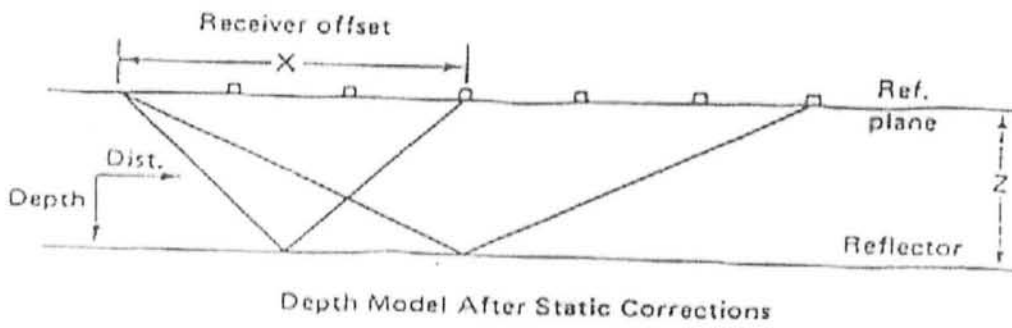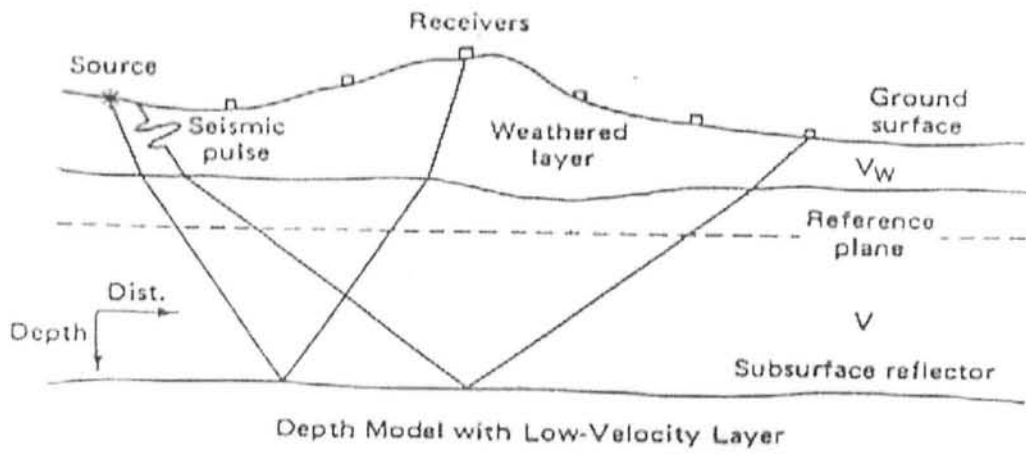
Figure 3.2 Diagrammatic representations of Static corrections
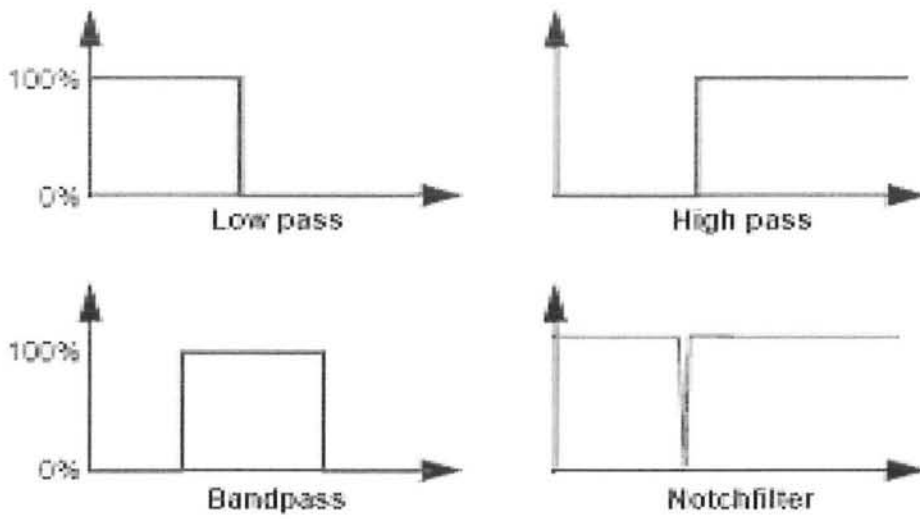
Figure 3.3 Types of Filters

1. Filtering

2. Deconvolution

3. Velocity Analysis (Yilmaz; 2001).

3.5a Filtering

Filtering is an operation by which the amplitude and/or phase spectrum of a time signal are altered. The aim of filtering is to improve signal to noise ratio. There are two basic methods of filtering:

- Frequency Domain Method
- Time Domain Method

Other special designed filters are based on one parameter as a basis of filtering e.g. velocity filters, fk-filters, and т-p filters, dip filters etc.(Kearey, Brooks & Hill; 2002, Yilmaz; 2001).

3.5b Deconvolution

It is a filtering process designed to improve resolution and suppress multiple reflections (Dobrin & Savit; 1976).

Key parameters for Deconvolution are:

- Type of Deconvolution-spiking or prediction
- Portion of trace to be the source of the autocorrelation
- Length of filter operator
- White noise factor

3.5c Velocity Analysis

Velocity analysis is done to find the velocity that flattens a reflection hyperbola, which returns the best result when stacking is applied.

There are different ways to determine the velocity:

- (t2-x2)-Analysis.
- Constant velocity stack.

Constant velocity panels (CVP).

The NMO-correction is applied for a CMP using different constant velocities. The results of the different velocities are compared and the velocity that results in a flattening of the hyperbolas is the velocity for a certain reflector.

Constant velocity stacks (CVS):

The data is NMO-corrected. This is carried out for several CMP gathers and the NMO-corrected data is stacked and displayed as a panel for each different stacking velocity. Stacking velocities are picked directly from the constant velocity stack panel by choosing the velocity that yields the best stack response at a selected event. Both methods can be used for quality control and for analysis of noisy data.

Velocity-Spectrum The velocity spectrum is obtained when the stacking results for a range of velocities are plotted in a panel for each velocity side by side on a plane of velocity versus two-way travel-time. This can be plotted as traces or as iso-amplitudes (Yilmaz; 2001)

3.6. MIGRATION:

Migration moves dipping reflectors in to their true subsurface position and collapse diffraction, thereby delineating detailed subsurface feature such as fault planes.

The goal of migration is to make the stacked section appear similar to geological cross section along the seismic line. Ideally we want to get a depth
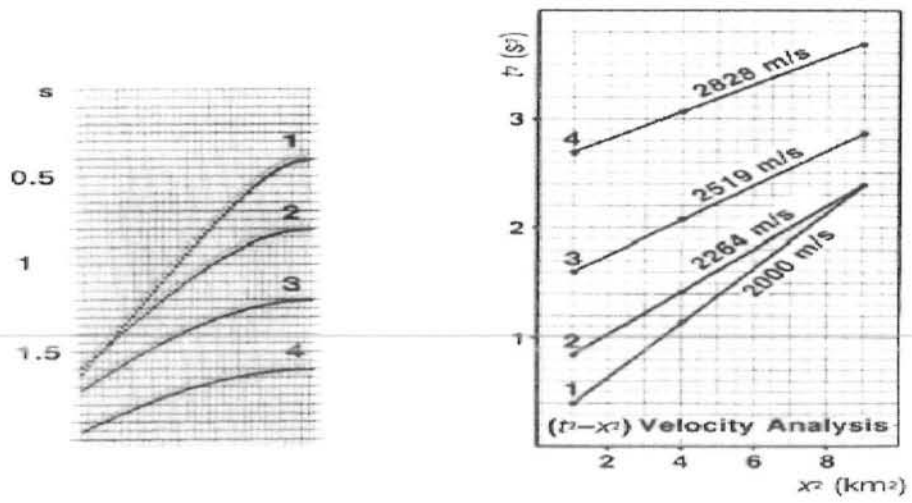
Figure 3.4 an Example of T2-X2 Analysis

section from the stacked section. However, the migrated section commonly displayed in time, one reason is that velocity estimated based on seismic and the other data always is limited accuracy. Therefore, depth conversion is not completely accurate.

The migration that produces a migrated time section is called time migration. In time migration we assume that velocity varies only in the vertical direction. But when the lateral velocity gradient are significant, time migration does not produce true subsurface picture. We need, Depth migration, the output of which is a depth section.

Types of Migration:

With respect to the stage when migration is applied on the seismic data during processing, there are two important types of migration.

- Pre-Stack Migration.
- Post-Stack Migration

Pre-Stack Migration:

Migration before stack is done to avoid the reflection point smearing of dipping reflections and to accommodate strong lateral velocity gradients.

Post-Stack Migration:

It is the Migration of stacked data, just like done before stacking.

3.7 Data Interpretation:

Deriving a simple and plausible model geologic model that is compatible with all observed data is referred as interpretation.

In seismic methods measurements are made at the surface by using different geophysical instruments which are then interpreted in terms of what might be in the subsurface. The behavior of different interfaces which give rise to reflection events is calculated from arrival reflection events is calculated from arrival times of seismic waves from these interfaces. (Sheriff; 1999).

(1) First of all we have to seismic section by considering the prominent horizons present. In this regard, well tops data would be very helpful. Below shown is the well tops data present in the area.

The data of well tops which is helpful in the conformation of the reflectors marked on the horizons is indicated in appendix.

(2) By considering the velocity files usually provided at the top of the section a time section of that. For those purpose R.M.S values of velocity is usually required (Figure 4.7)

(3) By considering the average velocity values draw a depth section from it by multiplying it with one way time i.e.

$$D = V_{AVG} * T/2$$

(4) Finally prepare contour map by considering the navigation data files of the area to be studied (i.e. Sinjhoro).

The navigation data of the seismic lines of study area is provided in the appropriate appendices.

CHAPTER # 04

INTERPRETATION

Chapter 04

INTERPRETATION

4.1 Introduction:

Seismic interpretation is the transformation of seismic reflection data into a structural picture, contouring of subsurface horizons and further depth conversion by applying some suitable velocities (Dobrin and Savit; 1988).

The present dissertation is concerned with the interpretation of seismic line 2001-SNJ-02 that lies in Sinjhoro area of Sindh province. Sinjhoro area lies in the Sanghar District of Sindh Province. Geologically it is a part of Southern Indus Basin. Ten discoveries have been made in Sinjhoro out of the sixteen exploratory wells drilled in the area (Orient Petroleum International Report; January 01, 2010).Due to acoustic impedance contrast five prominent horizons were marked on the seismic section.

By means of information provided on the seismic section time and depth sections were prepared and then further work on rock physics analysis as well as reflection coefficients could be done at the end of this chapter.

4.2 Methods for Interpretation of Seismic Data:

There are two main approaches for the interpretations of a seismic section which are:

- Structural Analysis
- Stratigraphic Analysis

43

Structural Analysis:

In structural analysis main emphasis is on the structural traps in which tectonic play an important role. Structural traps include the faults, folds anticline, pop up, duplex, etc.

Stratigraphic Analysis:

Stratigraphic analysis involves the delineating the seismic sequences, which present the different depositional units, recognizing the seismic facies characteristic with suggest depositional environment and analysis the reflection characteristic variation to locate the both stratigraphy change and hydrocarbon depositional environment .

Figure 4.1 shows the general interpretation Flow Chart indicating how we proceed from seismic section towards the seismic interpretation.

4.3 Seismic Section:

The output of a seismic reflection survey is called Seismic Section. It is prepared by plotting, side by side, all the stacked traces from a CDP reflection profile. Most importantly it points out some the features of a geologic cross-section.

The seismic section of line SNJ-02 of Sinjhoro area is considered as shown in the Base map. Different horizons marked on it showing the strong reflections and indicating the different geologic information. The strong reflections are the indicators of hard rocks.

Five horizons were picked up on the given Line SNJ-02 of the Sinjhoro area of Southern Indus Basin. The reflectors were strong enough to be picked due to variation in acoustic impedance that is eventually caused by changes in lithology.

Seismic Interpretation Flowchart

1. Correlate seismic reflections with local stratigraphy (picking).

2. Track marker reflections throughout the available data.

3. Resolve misties between lines.

4A. Determine the signature of desired feature by modelling.

4B. Post time (or estimated depth) values to maps and contour. Often, *isochrons* (time difference values) are used instead.
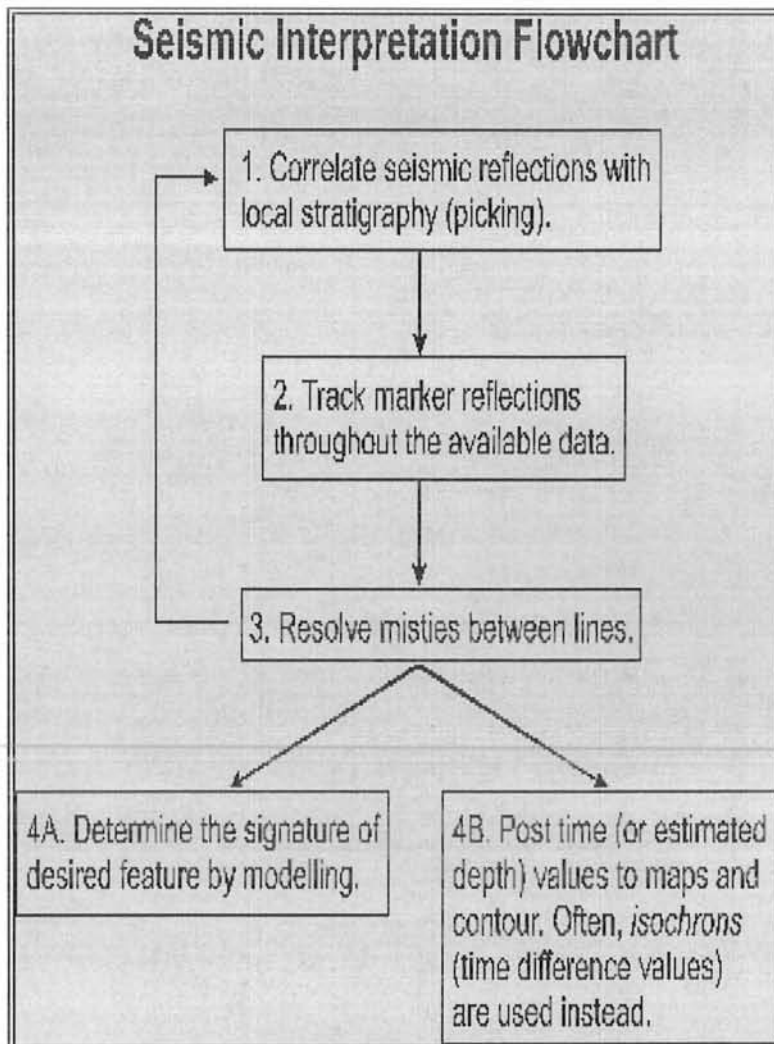
Figure 4.1 General Interpretation Flowchart

Along with five Reflectors R1, R2, R3, R4 and R5 from SP's 760-1100 two normal faults F1 & F2, are also marked on seismic section by seeing change in the reflectors character.

Velocity Variation

Velocity variation is basically concerned with the information of the velocities given in the upper part of seismic section. Five velocity windows are given on the section from SP's 760-1100 showing Root Mean Square, interval and average velocities of different subsurface layers at different times as shown in figures.4.2a, 4.2b and 4.2c respectively.

In the velocity window, the RMS velocity and interval velocity with respect to their respective times are given in the table, with the help of Vrms and Vint. , we are able to calculate the average velocity by using the DIX average velocity formula.

$$V_{n,av} = \frac{V_{n,int}(T_n - T_{n-1}) + V_{n,av} * T_{n-1}}{T_n}$$

Where

Vav   = average velocity (in m/s),

Vint   = interval velocity (in m/s) and

T   = zero of set travel time (in seconds).
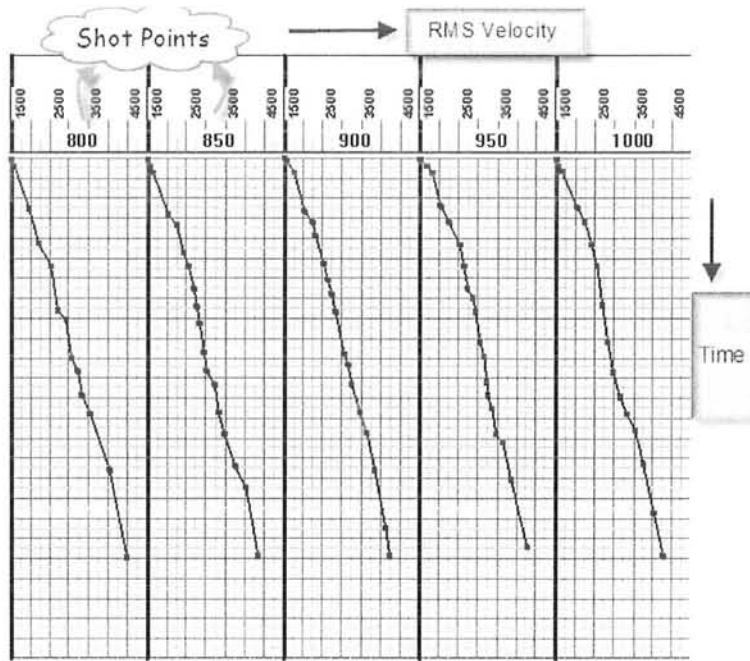
Figure 4.2a Variation in rms velocity with time for the given shot points
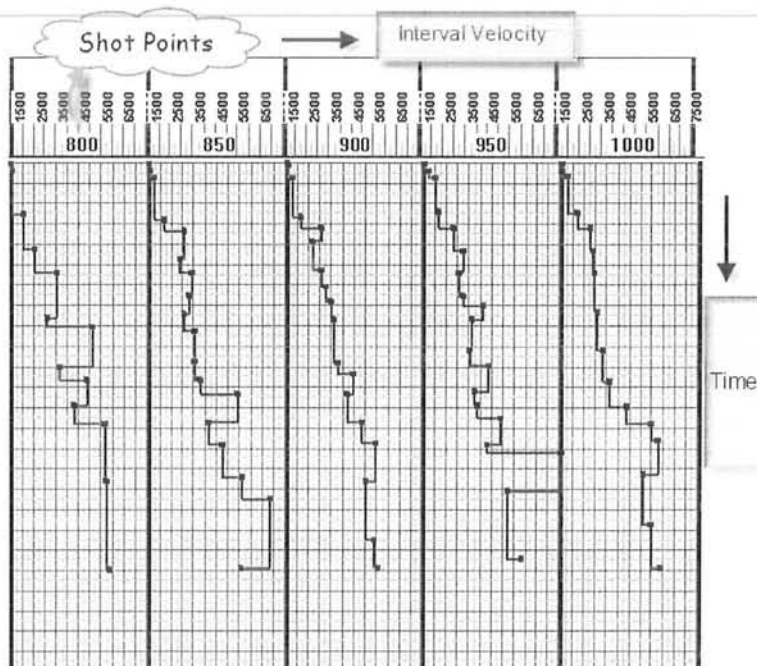
(SP: 760-1100)

Figure 4.2b Variation in interval velocity with time for the given shot points
(SP: 760-1100)
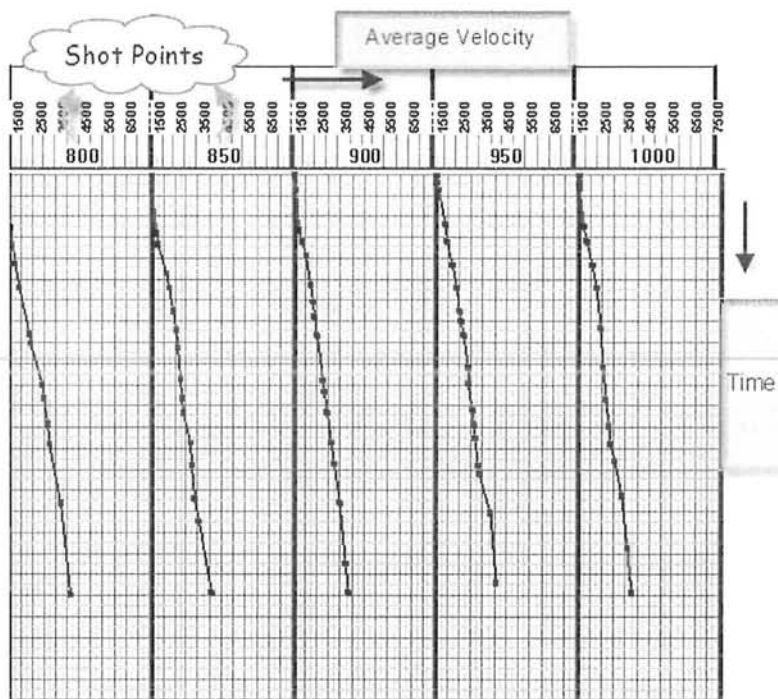
Figure 4.2c Variation in average velocity with time for the given shot points

(SP: 760-1100)

Interval Velocity

Interval velocity is the average velocity over some interval of travel path of the wave (Sheriff; 1999).

If two reflectors at depths 'z1' and 'z2' give reflections having respective one way times of 't1' and 't2', the interval velocity 'Vint' between the 'z1' and 'z2' is defined simply as

$$Vint = (z2 - z1) / (t2 - t1)$$

The individual layer velocities are called interval velocities because they indicate the specific reflectors.

Average Velocity

Average velocity (Vav) is simply the ratio of the depth (Z) of the reflector to one way zero off set travel time (T) of the seismic wave, that is

$$Vav = Z / T \text{ (Dobrin and Savit; 1998)}$$

Where,

Vav   = average velocity (m/s)

Z   = total thickness (in meters)

T   = total time (in seconds) up to that particular reflector whose average velocity is being calculate.

Average velocity is few percent smaller than the root mean square because it deals with layer thickness only not the path direction as in case of root mean square velocity. Interval velocity is used that is given in the velocity window to calculate the average velocity at specific interval of time for all the windows given in the section. (Sheriff; 1999)

Average Velocity Graph

Average velocity Graph is generated by plotting the values of average velocities on y-axis against the specific interval of time on x-axis. Graph is shown in Figure 4.3, which shows a simple relationship between the average velocity and time. Values of average velocity and time are given in appendix.

Mean average Velocity Graph:

This is simply calculated by dividing the sum of average velocities at constant intervals of time with the total number of observations so that

$$V_{mean} = (V_{ave\ 1}+V_{ave\ 2}+V_{ave\ 3}+\ldots\ldots+V_{ave\ n})\ /\ n$$

From these mean velocities the "Mean velocity Graph" can be made by plotting mean velocities against the time. From figure.4.4, it is seen that the velocity is increasing with the depth with time for the whole area under study.

Iso Velocity Graph:

Whenever the CDP's are plotted against the average velocities, a section formed which shows the lateral and vertical variations of the same velocity layers at different CDP's. The section so formed is termed as the Iso velocity section. This graph shows the push-up and pull-up velocities. These velocities are representative of variation of average velocities at certain time along different vibrating points. This variation represents the faults that are present in seismic section. The velocity variations are also because of coupling and thinning of high velocity material across the fault which causes velocity distortion. Iso velocity contour map for the given shot points is shown in figure 4.5.
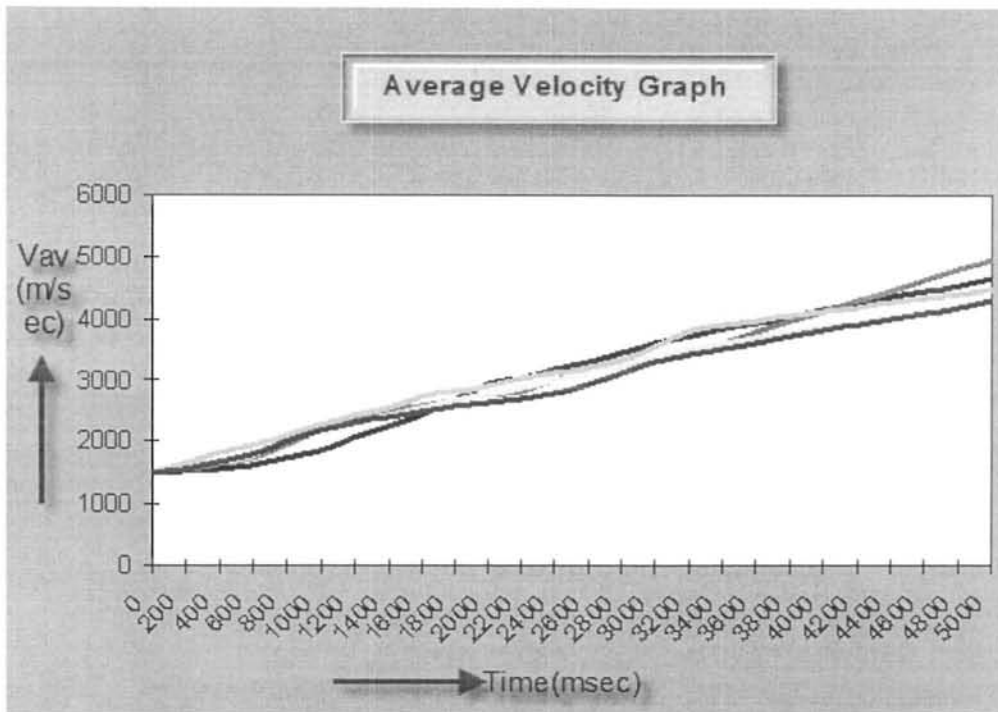
Figure 4.3 Average Velocity Graph of seismic line SNJ-02 (SP: 760-1100)
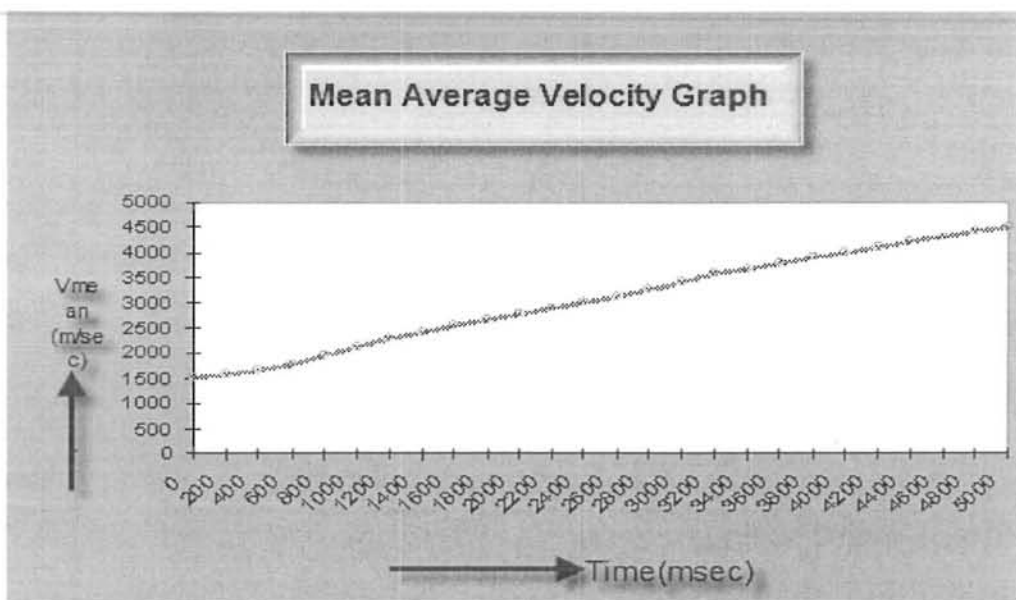
Figure 4.4 Mean Average Velocity Graph of seismic line SNJ-02 (SP: 760-1100)
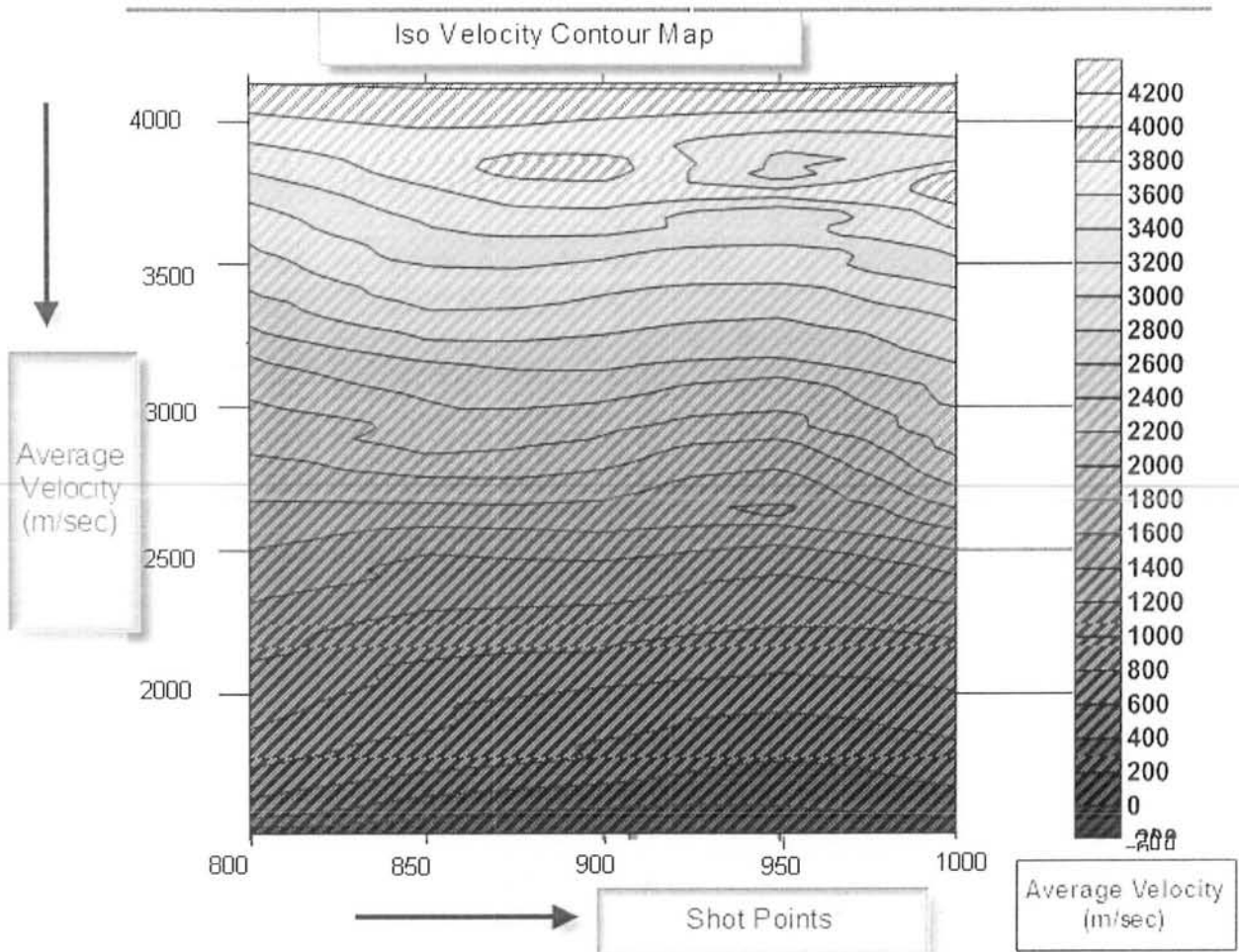
Figure 4.5 Iso Velocity Contour Map of seismic line SNJ-02 (SP: 760-1100)
showing horizontal and lateral variations in seismic velocities

4.4 Marking of Seismic Horizons:

The first step of interpretation process is to mark the reflectors. A reflector is defined as an interface or boundary between two rock units (formation). Those reflectors are selected which are real, show good character and continuity, and can be followed throughout the area. (Badely; 1985).

Five horizons are picked up on the line 2001-SNJ-02 of the Sinjhoro area. The reflectors were strong enough to be picked due to variation in acoustic impedance that is eventually caused by changes in lithology.

Reflectors Identification on the Seismic Section:

The identification of reflection packages has been done using the following;

- ➢ Depths of the formation tops from Chak 63-01.
- ➢ Using the average thickness of strata from above mentioned well.
- ➢ Using interval and average velocities derived during processing of seismic data.
- ➢ Geologic and seismic characteristics of different lithologies.
- ➢ Using tie point of two lines.

With the help of all these things discuss above four reflectors are marked

Results from the seismic section are:

Reflector 1

This reflector varies between SP 760 to SP 1100 at time ranges of 0.60 sec to 0.63 sec in the time section (Figure 4.6). The depth ranges from 540m to 570m in the depth section (Figure 4.7). It is named as **TOP OF LAKI FORMATION** on the basis of depth of formations encountered in well data.

Reflector 2

This reflector varies between SP # 760 to SP # 1100 at time ranges of 1.03 sec to 1.06 sec in the time section. The depth ranges from 1130 m to 1160m in the depth section. It is named as **TOP OF RANIKOT FORMATION** on the bases of depth of formations encountered in well data

Reflector 3

This reflector varies between SP # 760 to SP # 1100 at time ranges of 1.23 sec to 1.3 sec in the time section. The depth ranges from 1430 m to 1585m in the depth section. It is named as **TOP OF KHADRO FORMATION.**

Reflector 4

This reflector varies between SP # 760 to SP # 1100 at time ranges of 1.97 sec to 2.01 sec in the time section. The depth ranges from 2762 m to 2750 m in the depth section. It is named as TOP OF BASAL SAND.

Reflector 5

This reflector varies between SP # 760 to SP # 1100 at time ranges of 2.51 sec to 2.52 sec in the time section. The depth ranges from 3898 m to 3922 m in the depth section. It is named as **TOP OF CHILTAN LIMESTONE.**

4.5 TIME SECTION:

Time section is actually the reproduction of reflectors marked on the given processed seismic section. The time of each reflector is read from the Seismic section and then plotted against the shot points.

On the given seismic section five reflectors are marked as R1, R2, R3, R4 and R5 from top to bottom.

4.6 DEPTH SECTION:

The depth of each horizon can be calculated by their respective time and velocity by using the following relation

$$D = (T * V) / 2$$

Where,

D = Depth

T = Two way reflection time

V = Dix average velocity (in meter/second)

Using this formula the depth is calculated at each vibrating point. This calculated depth is then plotted against V.P. to get the depth section as indicated in Figure 4.7.

4.8 CONTOUR MAPS:

"A line that is formed by connecting the points of equal values is called a contour line. A map that uses contour lines as its vehicle for illustration is called a contour map".

Contouring is the main tool used in the seismic interpretation. After contouring it becomes obvious that what sort of structure is forming a particular horizon. The **Basal Sand** is selected for the purpose of constructing contour maps because it is a producing reservoir in the Southern Indus Basin.
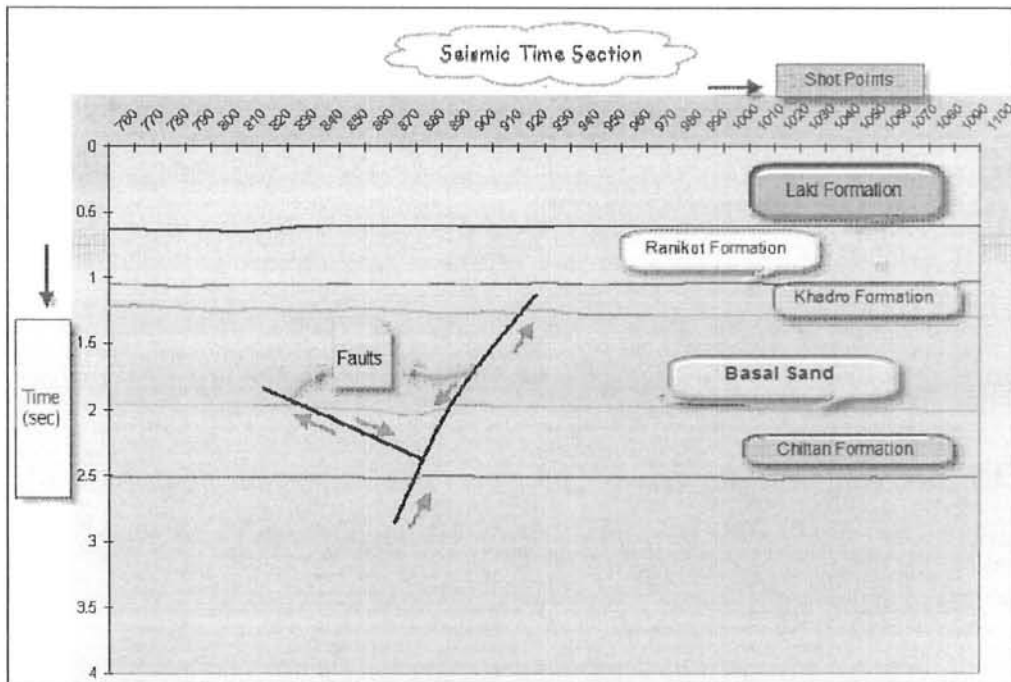
Figure 4.6 Time Section of seismic line SNJ-02 from SP: 760-1100
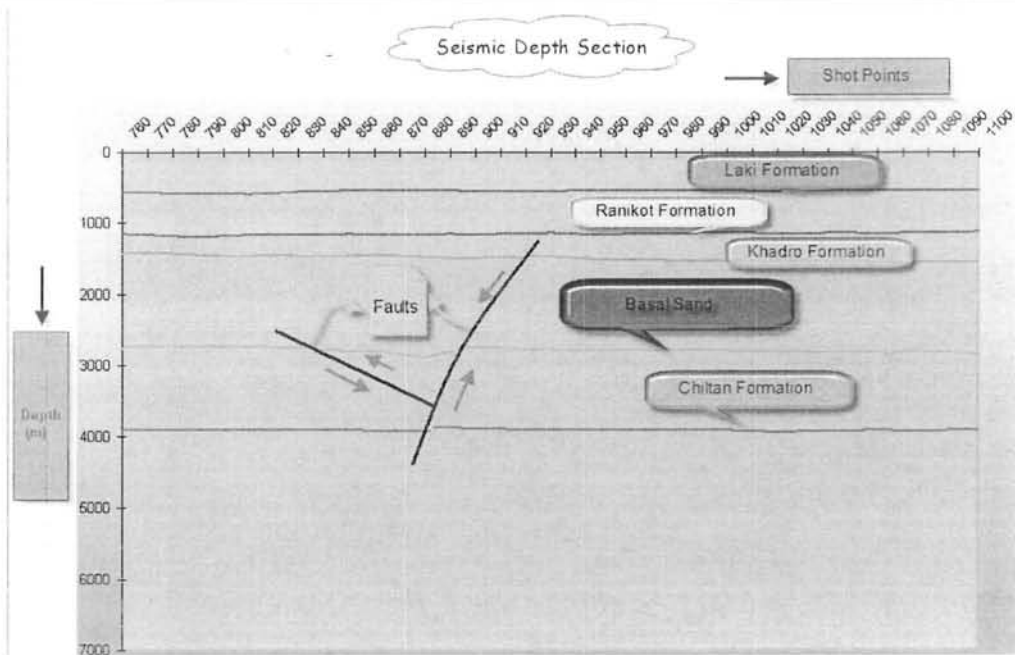
Figure 4.7 Depth Section of seismic line SNJ-02 from SP: 760-1100

Time Contour Map and Surface at Basal Sand level:

After the marking of the horizons at different levels, the next step is to contour the area at a particular level and prepare its surface. Here the first step is to note the time of Basal Sand Formation, for all the available seismic sections with respect to the vibrating points. Here the data of Lines is used for contouring which include **SNJ-02, SNJ-22, SNJ-17, SNJ-18, SNJ-19, SNJ-24** and **SNJ14.**Then the **EAST/NORT** for each vibrating point is noted from the base map and then using the **'SURFER'** the contour map is prepared. Where contours are closely spaced they show abrupt change in time to the Formation. The time contour map of Basal Sand is shown in Figure 4.8

The next step is to make the surface at that level. From the surface map of Basel Sand Formation anticline like structure can be seen and these are by using the same data that is used for the time contour mapping and the velocities additionally from the velocity windows, we note the velocities for each vibrating point at the Basal Sand level and then by multiplying the time with velocity and dividing by two to get the depth at each vibrating point. Then using the same procedure that is used in the preparation of the time contour maps and the surface, the depth contour map and the surface can be prepared. Where the contours are closed they show abrupt change in elevation. In the centre values of depth increases which shows probable synclinal structure in the Basal Sand Formation. Depth contour map of Basal Sand Formation is shown in the figure 4.10.
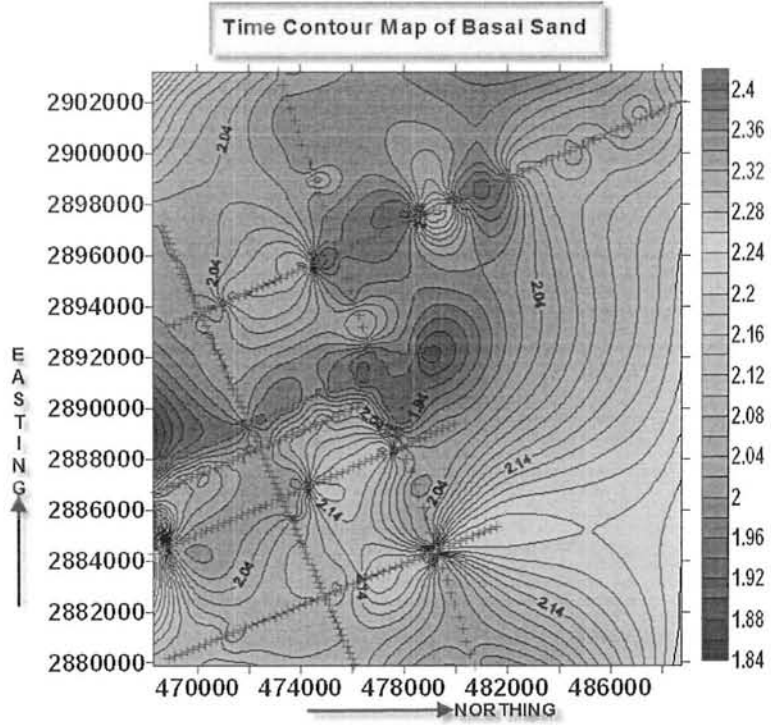
Figure4.8 Time Contour Map of Basal Sand
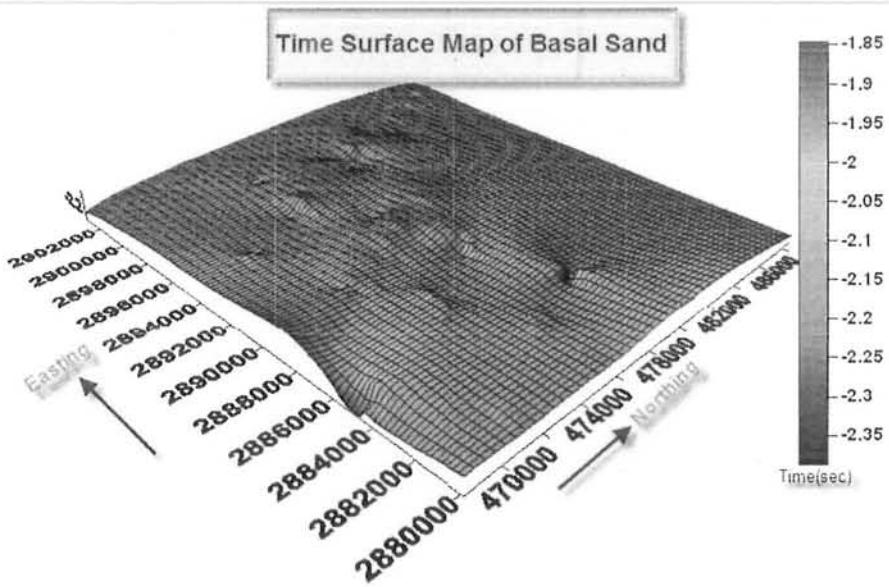
Figure 4.9 Time Surface Map of Basal Sand
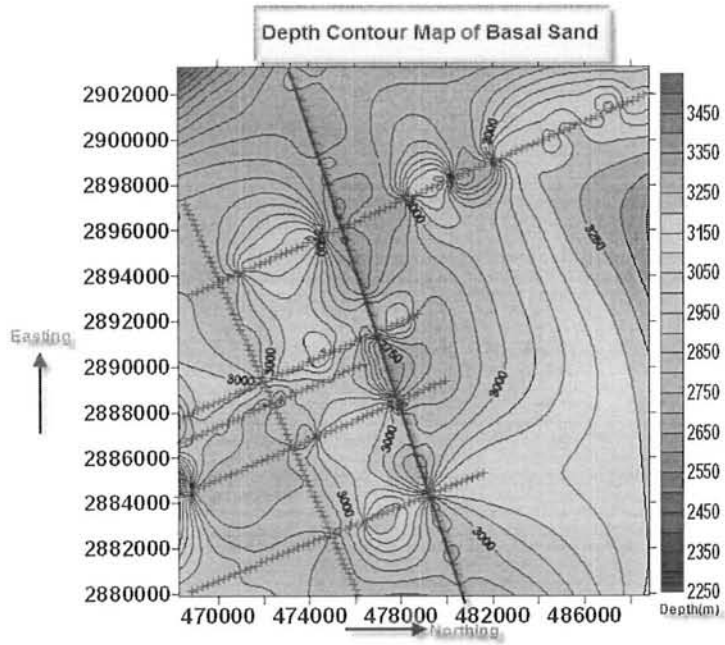
Figure4.10 Depth Contour Map of Basal Sand
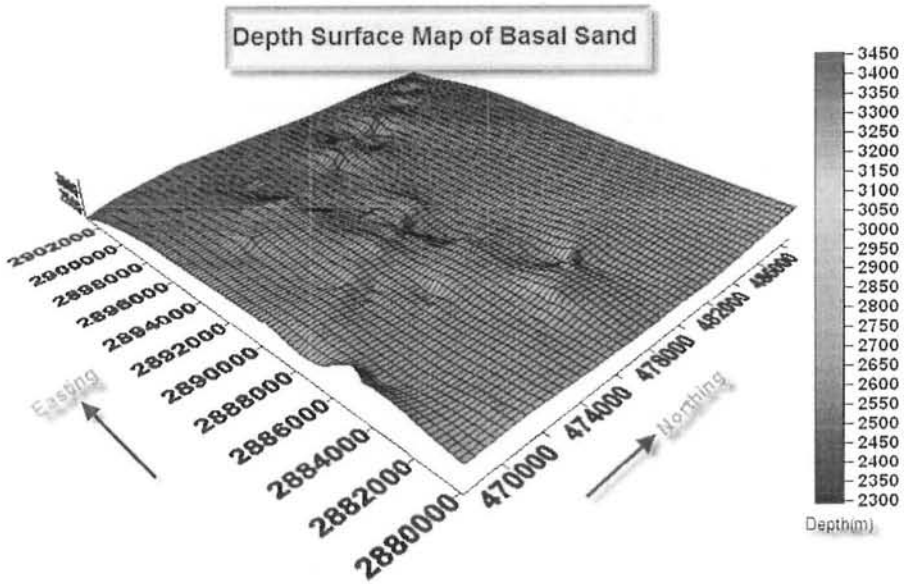
Figure 4.11 Depth Surface Map of Basal Sand

4.9 Introduction to Rock Physics:

Rock Physics is the investigation and study of the physical behavior and properties of the rocks in order to determine the physical properties of the rocks. Different relations are establishing between the material properties and the observed seismic response, so that properties may be detected seismically.

After the calculation of P-wave (Vp) velocity we are able to calculate the following relationships i.e.

Rock Parameters:

S-Wave Velocity (Vs):

It is calculated by the relation

$$V_s = (V_p - 1.36)/1.16$$

Density (ρ):

Mass per unit volume is called density. The density of subsurface rock is calculated by the following relation as p-wave velocity is known.

$$\rho = 0.31 * V_p^{.25}$$

Where

ρ = density of rock unit.

Vp = velocity of P-wave.

As the density of hydrocarbons is much low, so the zones of low density may indicate hydrocarbons or other less dense materials.

Shear Modulus (μ):

Shear modulus (μ) is defined as the ratio of shear stress to the shear strain (angle of deformation). Shear modulus is the measure of the ability of a rock body to resist the change in shape when forces are applied. Estimation of Shear Modulus from shear wave velocity and density have been done by using the formula

$$\mu = \rho V_s^{\,2}$$

Where

μ = shear modulus

Vs = shear wave velocity.

The value of shear modulus is Calculated on each CDP and given in appendix. If the value of shear modulus is high, then the rock unit is more fractured and more sheared.

Bulk Modulus (K):

The bulk modulus (K) measures the substance's resistance to uniform compression. It is the ratio of volume stress to volume strain. Bulk modulus is the measure of the ability of a rock body to resist the change in volume In order to find the Bulk Modulus (K) the relation use is

$$K = \rho \left(V_p^{\,2} - \frac{4}{3} V_s^{\,2} \right)$$

Where

K = bulk modulus

ρ = density of rock.

If the value of K is infinity (∞), then material is said to be incompressible. On the other hand, if the value of K is zero (0), then the material can be easily compressed.

Poisson's Ratio   (σ):

It is the ration of transverse strains to the longitudinal strain. It can also be expressed as

$$\sigma = 0.5(V_p^2 - 2V_s^2)/(V_p^2 - V_s^2)$$

The above formula approximates the trend of seismic velocities because it is a function of P-wave and S-wave velocity. Poisson Ratio has a range

$$-1 \leq \sigma \leq 0.5.$$

Vp Vs Ratio

The Vp/Vs ratio is calculated using the following relation

$$VpVs_{Ratio} = \sqrt{\frac{K}{\mu} + \frac{4}{3}}$$

The above formula is a function of Bulk modulus and Shear modulus. The Bulk modulus is a measure of compressibility while Shear modulus is a measure of rigidity. It is used to determine the reservoir properties.

All the above relationships are calculated in the table given in appendix.

Depth VS Density:

Density is a major property of the rock, which describes the amount of solid part of the rock body per unit volume. Data for density and depth is shown in table in appendix.

Figure 4.12 shows the graph in which the depth (m) is plotted along x-axis and density (gm/cm3) along y-axis. The trend of graph shows that the density increases with depth. The density of crude oil is between 0.75 - 1.05g/cm3. It means that where the density lies in this range there are chances for the presence of crude oil.

Depth VS Poisson ratio:

Poisson's Ratio is more dependent upon P-wave velocity rather than S-Wave velocity. Data for Poisson ratio and depth is shown in table in the appendix. Figure 4.13 shows graph the depth (m) is plotted along x-axis and Poisson Ratio is plotted along y-axis. The trend of graph shows that the fall in Poisson ratio has a gradual decrease with depth. The value of Poisson ratio lies in the range of

$$-1 \leq \sigma \leq 0.5.$$

Depth versus Vp/Vs Ratio:

Vp/Vs ratio is the combined behavior of Bulk modulus and Shear modulus. Data for VpVs ratio and depth is shown in table.

Figure 4.14 shows graph the depth (m) is plotted along x-axis and Vp Vs ratio is plotted along y-axis. The trend of the graph shows that, the ratio become higher at first and then decreases downward relatively.
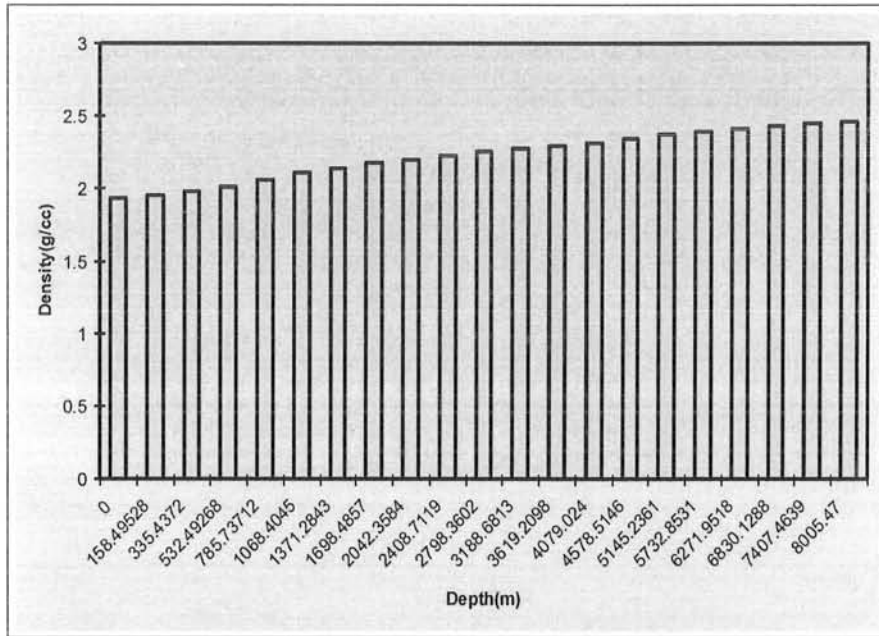
Figure 4.12 Graph for Depth Vs Density showing apparent increase in density with depth due to overlying lithostatic pressure
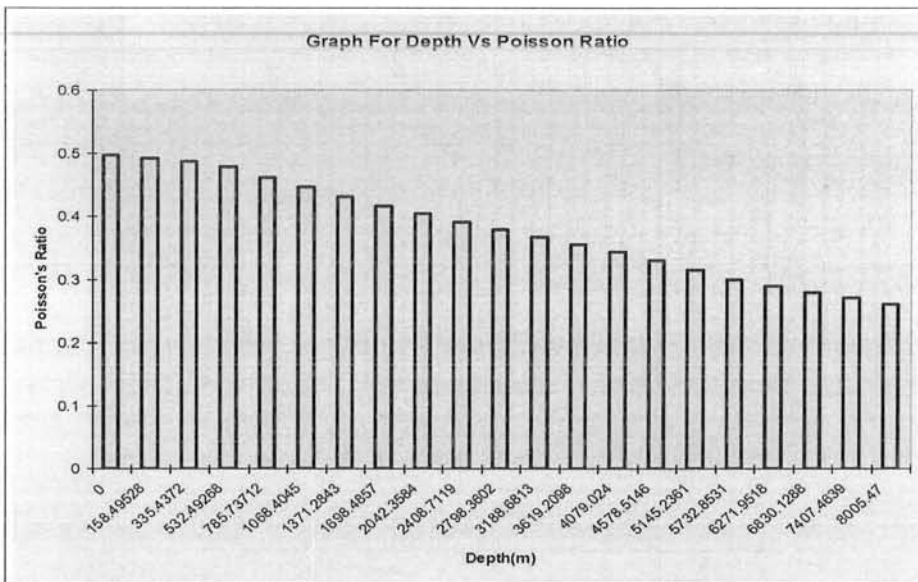
Figure 4.13 Graph for Depth VS Poisson Ratio showing an apparent decrease in poisson ratio with depth
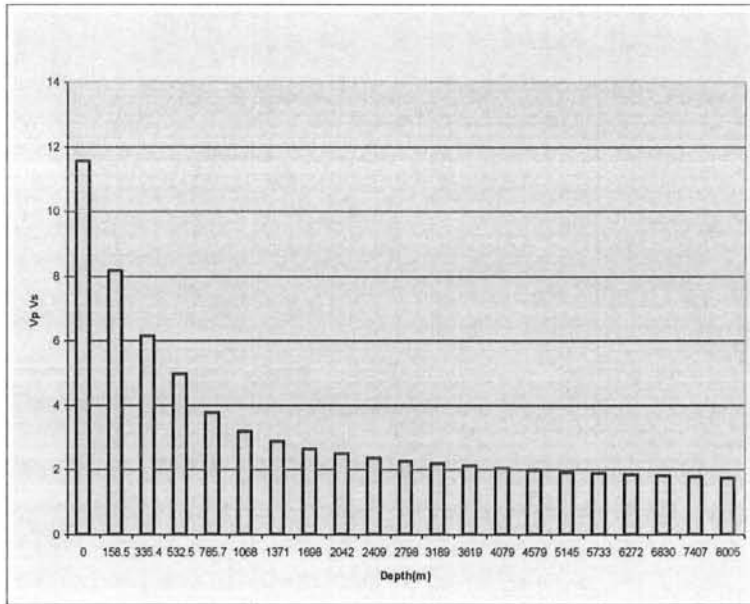
Figure 4.14 Graph for Depth versus VpVs Ratio showing general decreasing trend of Vp Vs ratio with depth
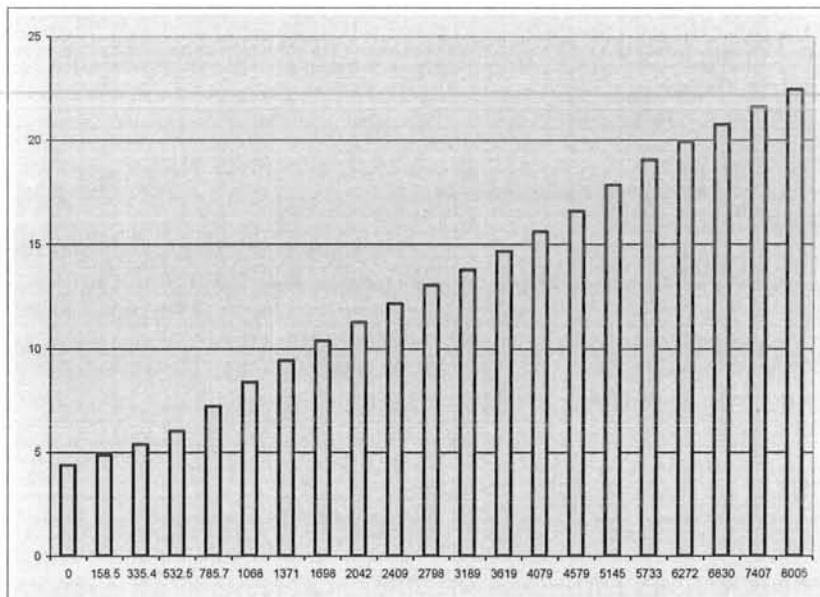
Figure 4.15 Graph for Bulk Modulus Vs Depth indicating an increasing trend of Bulk modulus with depth
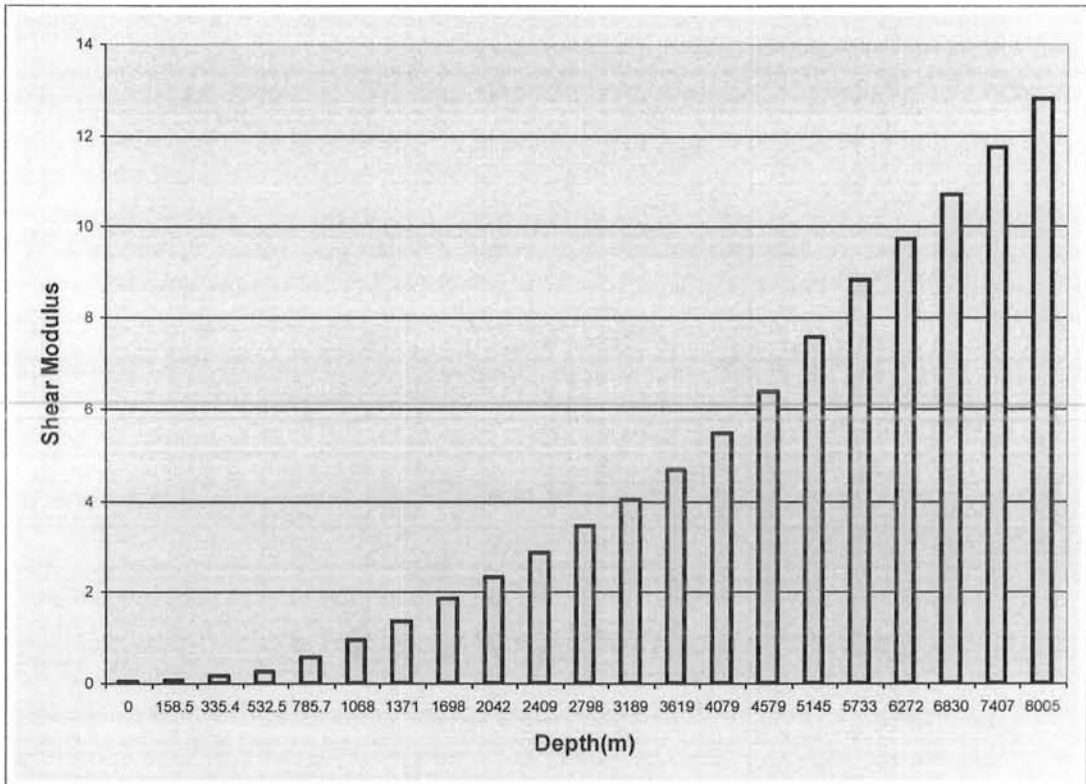
Figure 4.16 Graph for Shear Modulus Vs Depth showing an increasein value of shear modulus with depth

4.10 Identification of Lithology on the basis of Reflection Coefficient:

Reflection Coefficient is the measure of the strength of the reflected wave. It is calculated by subtracting the acoustic impedances of two layers and then dividing them on their sum.

For the specific case of normal incident (ray path perpendicular to interface) there is simple equation relating the incident amplitude to the reflected amplitude. The ratio is called the "reflection coefficient", R.

$$R = (V2 \, \rho2 - V1 \, \rho1) / (V2 \, \rho2 + V1 \, \rho1)$$

Where

$\rho2$ = Density in second Interval

V2 = Velocity in second Interval

$\rho1$ = Density in first Interval

V1 = Velocity in first interval (Zia-ur-Rehman; 1988).

The Range of Reflection Coefficient values are used.

Reflection Coefficient Range	Lithology
Greater Than 0.06	Limestone
0.01 – 0.06	Sandstone
Less Than 0.01	Shale

Table 4.1 Reflection Coefficient Range

Density is calculated by using interval velocities. Figs. 4.17-4.21 show the presence of limestone, sandstone and shale in the subsurface corresponding to the given source points. Limestone lies in the area that has reflection coefficient

67

higher than 0.06. Sandstone lies in the area where reflection coefficient is higher than and equal to 0.01 but less than equal to 0.06.Shale lies in the area where reflection coefficient is less than 0.01.

Brown color represents the limestone; Orange represents the Sandstone & Yellow represent the Shale.

With the help of figures below we can easily determined the lithology on the basis of reflection coefficients. The variation in the values of Reflection Coefficient have indicated the presence of Limestone, Sandstone and Shale in subsurface. There is a change in phase and we have a negative polarity which gives the indication of shale. The confirmation with the help of well data was not possible because of the non availability of the well data.
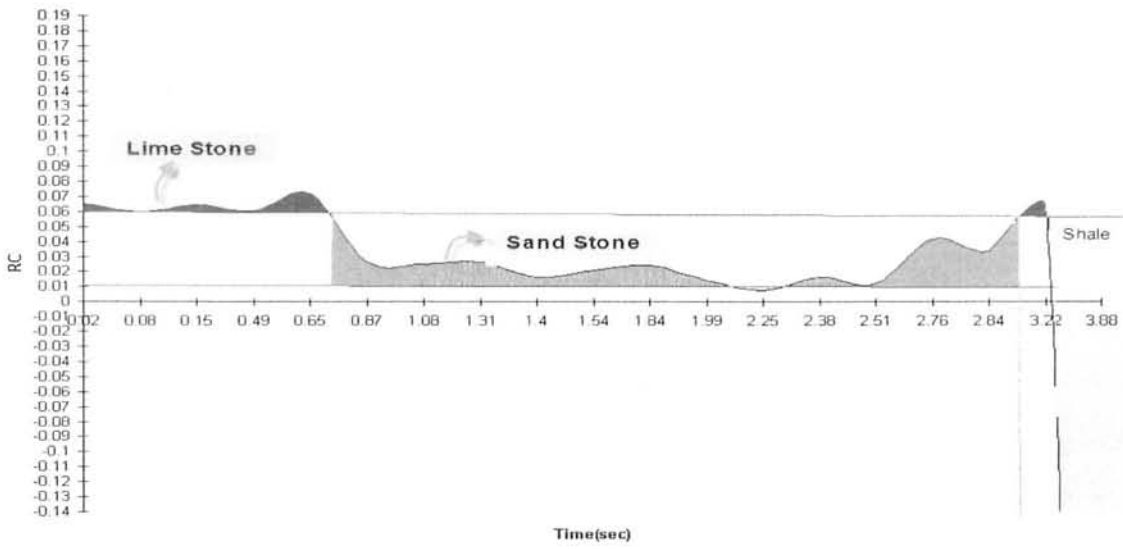
Figure 4.17 Reflection Coefficient Vs Time for SP-800
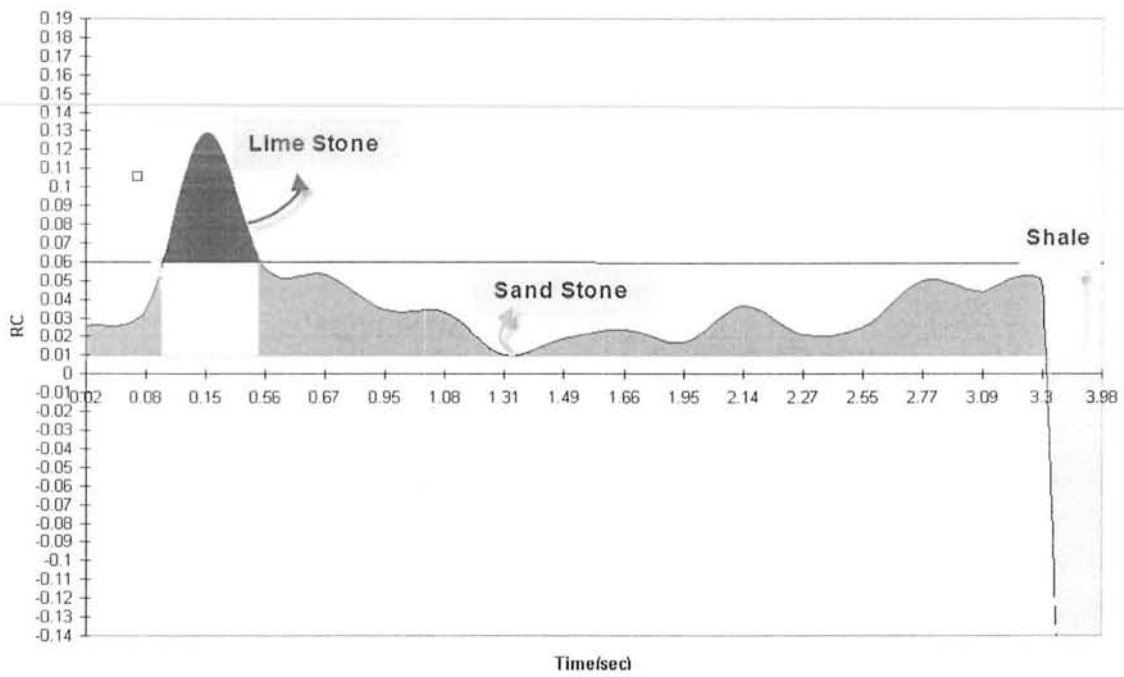
Figure 4.18 Reflection Coefficient Vs Time for SP-850
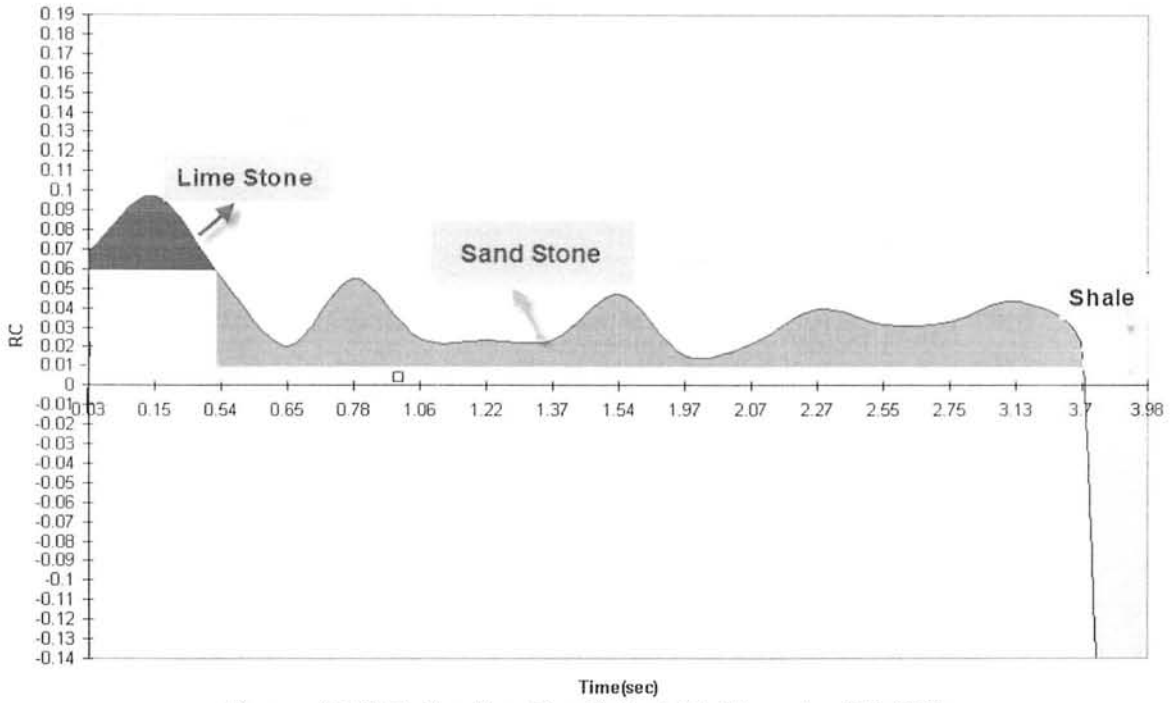
Figure 4.19 Reflection Coefficient Vs Time for SP-900
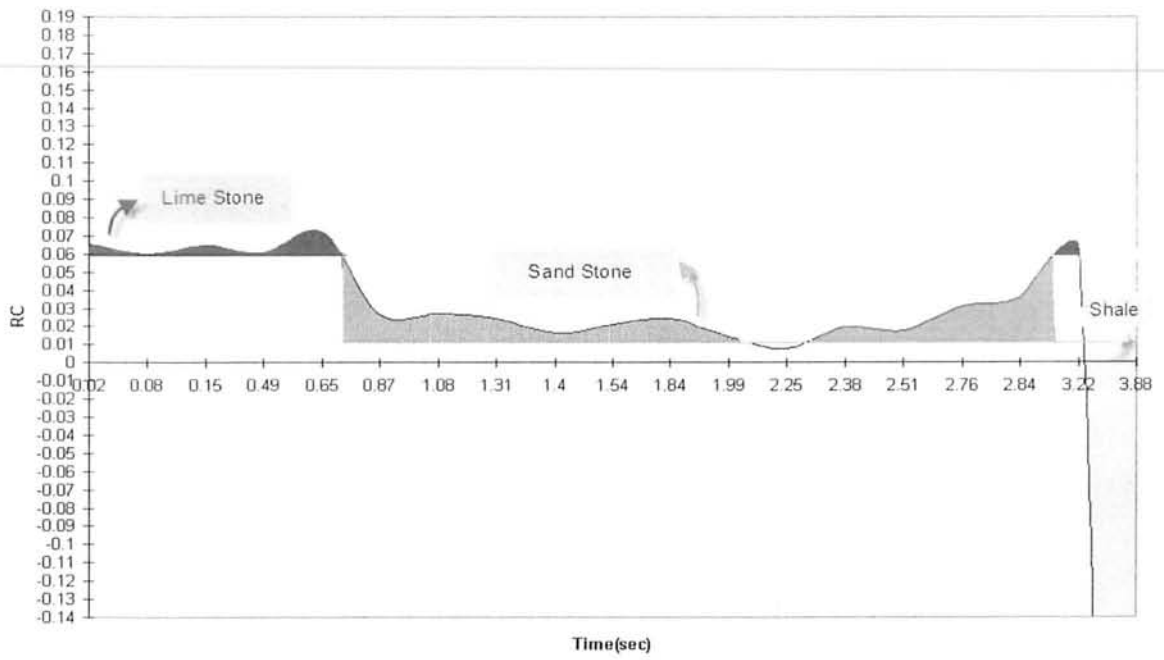
Figure 4.20 Reflection Coefficient Vs Time for SP-950
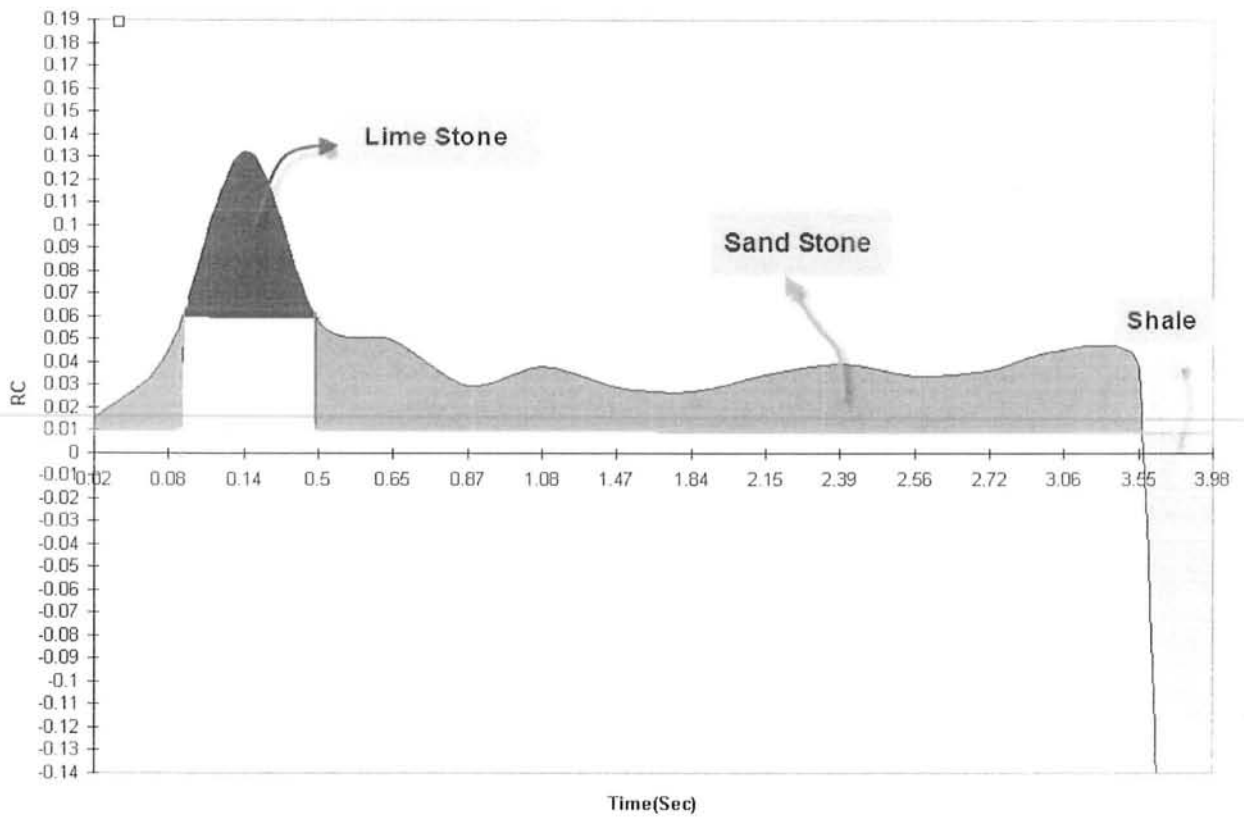
Figure 4.21 Reflection Coefficient Vs Time for SP-1000

It is to be noted that the position of lithologies indicated by reflection coefficient figures are somewhat deviating as indicated by time section.The probable reason of that is the limition as well as reliability of data provided.

Conclusions:

After interpreting the given seismic section, following conclusions are made:

- On the basis of seismic data five horizons have been identified.
- Horizons are marked on the basis of continuity and character of seismic traces.
- For structural interpretation two faults marked on the seismic section between SP's 760-1100. Both are normal faults. As Normal faults are the extensional feature it means that extension takes place in the study area.
- The first Normal Fault is in between SP's 830-890 and the second Normal Fault which displaces the three formations is in between SP's 840-920.
- For velocity variation, Iso-velocity map have been prepared. Vertical change of velocity in the Iso-Velocity Map is due to the change in density and lithology of the strata. Whereas, the horizontal change in velocity is due to folding and faulting.
- The variation in the values of Reflection Coefficient have indicated the presence of Limestone, Sandstone and Shale in subsurface.
- Other physical properties like Density, Bulk Modulus (k), Shear modulus (μ), Poisson's Ratio (σ), Lame's Parameter (λ), and Acoustic Impedance are calculated and shown in the appendix.
- The values of Poisson's ration lies in the range -1 to 0.5.

APPENDIX

Time (msec)	Vav (S.P 1600)	Vav (S.P1700)	Vav (S.P 1800)	Vav (S.P1900)	Vav (S.P 2000)
0	1514	1512	1512	1512	1510
200	1533.015	1569.808	1603.188	1655.203	1563.55
400	1564.707	1645.271	1682.639	1821.461	1671.852
600	1631.337	1733.442	1776.635	1936.006	1797.458
800	1740.668	1954.721	2022.396	2099.645	2004.284
1000	1873.497	2186.534	2145.492	2293.27	2185.252
1200	2055.473	2347.08	2282.454	2433.383	2308.979
1400	2263.501	2497.479	2419.702	2539.884	2411.475
1600	2423.212	2582.602	2548.29	2715.188	2495.448
1800	2672.723	2665.977	2656.158	2817.429	2569.446
2000	2940.265	2753.879	2762.48	2896.21	2638.967
2200	3033.725	2831.076	2889.73	3029.376	2710.099
2400	3184.597	2991.125	3005.565	3107.044	2791.71
2600	3286.07	3158.949	3113.982	3199.989	2929.564
2800	3439.432	3233.394	3247.79	3317.761	3113.461
3000	3592.794	3333.711	3391.75	3542.358	3290.174
3200	3725.548	3455.308	3515.292	3805.216	3413.802
3400	3827.388	3608.962	3600.919	3894.969	3514.679
3600	3929.229	3777.264	3686.546	3965.489	3614.052
3800	4031.069	3945.565	3771.774	4036.009	3708.909
4000	4132.909	4113.867	3856.605	4106.528	3803.766
4200	4234.75	4282.168	3941.436	4177.047	3898.623
4400	4336.59	4450.47	4026.266	4247.567	3993.48
4600	4438.431	4618.771	4111.097	4318.086	4088.337
4800	4540.271	4787.072	4195.928	4388.606	4183.194
5000	4642.111	4955.374	4280.758	4459.125	4278.051

1.1 Data for Average Velocity Graph

Time(msec)	Mean Velocity(m/sec)
0	1512
200	1584.9528
400	1677.186
600	1774.9756
800	1964.3428
1000	2136.809
1200	2285.4738
1400	2426.4082
1600	2552.948
1800	2676.3466
2000	2798.3602
2200	2898.8012
2400	3016.0082
2600	3137.7108
2800	3270.3676
3000	3430.1574
3200	3583.0332
3400	3689.3834
3600	3794.516
3800	3898.6652
4000	4002.735
4200	4106.8048
4400	4210.8746
4600	4314.9444
4800	4419.0142
5000	4523.0838

1.2 Data for Mean Velocity Graph

SP-800	SP-850	SP-900	SP-950	SP-1000
Vavg(m/s)	Vavg(m/s)	Vavg(m/s)	Vavg(m/s)	Vavg(m/s)
1514	1512	1512	1512	1510
1517.169	1523.126	1553.607	1541.04	1517.02
1533.015	1569.808	1603.188	1655.203	1563.55
1548.861	1607.539	1642.913	1738.332	1617.701
1564.707	1645.271	1682.639	1821.461	1671.852
1580.553	1683.002	1722.364	1899.889	1726.003
1631.337	1733.442	1776.635	1936.006	1797.458
1686.003	1821.931	1886.106	2002.591	1890.218
1740.668	1954.721	2022.396	2099.645	2004.284
1802.047	2087.512	2083.944	2196.587	2107.466
1873.497	2186.534	2145.492	2293.27	2185.252
1951.459	2256.794	2211.001	2381.078	2257.731
2055.473	2347.08	2282.454	2433.383	2308.979
2159.487	2437.366	2351.324	2485.689	2360.227
2263.501	2497.479	2419.702	2539.884	2411.475
2367.515	2551.658	2488.436	2643.192	2458.449
2423.212	2582.602	2548.29	2715.188	2495.448
2538.952	2619.685	2602.224	2766.309	2532.447
2672.723	2665.977	2656.158	2817.429	2569.446
2806.494	2712.268	2710.092	2858.547	2604.766
2940.265	2753.879	2762.48	2896.21	2638.967
2973.207	2790.811	2818.112	2962.793	2673.168
3033.725	2831.076	2889.73	3029.376	2710.099
3112.626	2890.888	2955.025	3077.305	2749.759
3184.597	2991.125	3005.565	3107.044	2791.71
3228.848	3091.362	3056.105	3138.633	2854.283
3286.07	3158.949	3113.982	3199.989	2929.564
3362.751	3193.889	3179.194	3264.652	3023.907
3439.432	3233.394	3247.79	3317.761	3113.461
3516.114	3283.552	3319.77	3410.929	3201.818
3592.794	3333.711	3391.75	3542.358	3290.174
3669.476	3385.804	3463.729	3673.787	3363.364
3725.548	3455.308	3515.292	3805.216	3413.802
3776.468	3524.812	3558.106	3859.71	3464.241
3827.388	3608.962	3600.919	3894.969	3514.679
3878.309	3693.113	3643.732	3930.229	3565.118
3929.229	3777.264	3686.546	3965.489	3614.052
3980.149	3861.415	3729.359	4000.749	3661.48
4031.069	3945.565	3771.774	4036.009	3708.909
4081.989	4029.716	3814.189	4071.268	3756.337
4132.909	4113.867	3856.605	4106.528	3803.766

1.3 Data for Iso Velocity Graph

P	Time1(sec)	Time 2(sec)	Time 3(sec)		Time 4(sec)			Time 5(sec)	
760	0.63	1.05	1.23		1.97			2.52475	
770	0.63	1.06	1.22		1.97			2.52225	
780	0.64	1.07	1.23		1.97			2.52025	
790	0.64	1.08	1.24		1.97			2.52275	
800	0.64	1.07	1.25		1.97			2.52475	
810	0.65	1.06	1.25		1.9705			2.52225	
820	0.64	1.06	1.24		1.9755			2.52025	
830	0.62	1.06	1.25		1.98			2.52275	
840	0.61	1.06	1.25			1.993571		2.525	
850	0.605	1.05	1.25			2		2.525	
860	0.604	1.06	1.24			2.0025		2.525227	
870	0.604	1.06	1.25			2.0275		2.5275	
880	0.604	1.06	1.26			2.045833		2.529773	
890	0.605	1.05	1.27			2.004167			2.512353
900	0.61	1.06	1.27				1.98		2.5154
910	0.61	1.05	1.26				1.99		2.5194
920	0.61	1.05	1.27				1.99		2.5231
930	0.61	1.04		1.25			1.99		2.5241
940	0.605	1.05		1.27			1.99		2.525
950	0.606	1.06		1.28			1.99		2.525
960	0.606	1.05		1.28			1.99		2.52475
970	0.605	1.05		1.28			1.99		2.52225
980	0.605	1.05		1.29			1.995		2.52025
990	0.604	1.04		1.29			1.995		2.52275
1000	0.606	1.04		1.29			2		2.5255
1010	0.607	1.04		1.29			2		2.5305
1020	0.607	1.05		1.29			2.01		2.53475
1030	0.605	1.05		1.29			2.01		2.53225
1040	0.603	1.04		1.29			2.01		2.52975
1050	0.603	1.04		1.29			2.01		2.52725
1060	0.603	1.05		1.3			2.01125		2.52525
1070	0.601	1.04		1.3			2.001875		2.52775
1080	0.6	1.04		1.3			2.01		2.5295
1090	0.6	1.04		1.3			2.01125		2.5245
1100	0.6	1.03		1.3			2.01		2.523

1.4 Data for time section

SP	Depth1(m)	Depth2(m)	Depth3(m)		Depth4(m)			Depth5(m)	
760	568.8	1154	1433		2767			3910	
770	568.8	1169	1417		2742			3904	
780	579.7	1184	1433		2742			3900	
790	579.7	1199	1449		2742			3904	
800	579.7	1184	1465		2742			3910	
810	590.7	1169	1465		2742			3904	
820	579.7	1169	1449		2752			3898	
830	558	1169	1465		2762			3904	
840	547.2	1169	1465			2786		3910	
850	542	1154	1465			2800		3912	
860	540.8	1169	1449			2800		3914	
870	540.8	1169	1465			2847		3916	
880	540.8	1169	1482			2894		3921	
890	542	1154	1498			2816			3880
900	547.2	1169	1498				2763		3887
910	547.2	1154	1482				2763		3896
920	547.2	1154	1498				2781		3905
930	547.2	1139		1474			2781		3907
940	542	1154		1498			2781		3910
950	542.9	1169		1514			2781		3910
960	542.9	1154		1514			2781		3910
970	542	1154		1514			2781		3904
980	542	1154		1531			2781		3898
990	540.8	1139		1531			2791		3904
1000	542.9	1139		1531			2791		3910
1010	544	1139		1531			2800		3922
1020	544	1154		1531			2800		3934
1030	542	1154		1531			2819		3928
1040	539.7	1139		1531			2819		3922
1050	539.7	1139		1531			2819		3916
1060	539.7	1154		1547			2819		3910
1070	537.6	1139		1547			2813		3916
1080	536.5	1139		1547			2819		3922
1090	536.5	1139		1547			2824		3910
1100	536.5	1124		1547			2850		3898

1.5 Data for depth section

Time(sec)	Vp(m/sec)	Vp(km/sec)	Vs(km/sec)	Depth(m)	Density(g/cc)	Shear Modulus	Bulk Modulus'k'	VpVs ratio	Poisson Ratio
0	1512	1.512	0.131	0	1.933	0.033	4.375	11.54	0.496
0.2	1585	1.585	0.194	158.5	1.956	0.074	4.816	8.173	0.492
0.4	1677	1.677	0.273	335.4	1.984	0.148	5.383	6.134	0.486
0.6	1775	1.775	0.358	532.5	2.012	0.258	5.996	4.962	0.479
0.8	1964	1.964	0.521	785.7	2.064	0.56	7.217	3.77	0.462
1	2137	2.137	0.67	1068	2.108	0.945	8.363	3.191	0.446
1.2	2285	2.285	0.798	1371	2.143	1.364	9.377	2.865	0.431
1.4	2426	2.426	0.919	1698	2.176	1.839	10.36	2.639	0.416
1.6	2553	2.553	1.028	2042	2.204	2.331	11.25	2.482	0.403
1.8	2676	2.676	1.135	2409	2.23	2.871	12.14	2.358	0.39
2	2798	2.798	1.24	2798	2.255	3.467	13.03	2.257	0.378
2.2	2899	2.899	1.327	3189	2.275	4.003	13.78	2.185	0.368
2.4	3016	3.016	1.428	3619	2.297	4.682	14.65	2.113	0.356
2.6	3138	3.138	1.533	4079	2.32	5.449	15.58	2.047	0.343
2.8	3270	3.27	1.647	4579	2.344	6.358	16.6	1.986	0.33
3	3430	3.43	1.785	5145	2.372	7.556	17.84	1.922	0.314
3.2	3583	3.583	1.916	5733	2.398	8.808	19.05	1.87	0.3
3.4	3689	3.689	2.008	6272	2.416	9.742	19.9	1.837	0.29
3.6	3795	3.795	2.099	6830	2.433	10.72	20.74	1.808	0.28
3.8	3899	3.899	2.189	7407	2.45	11.73	21.59	1.781	0.27
4	4003	4.003	2.278	8005	2.466	12.8	22.44	1.757	0.26

1.6 Data for Finding the Reservoir Characteristics

SP-800				
Time (sec)	Vp (m/sec)	Density (g/cc)	Acoustic Impedence "Z"	Reflection Coefficient "RC"
0.02	1512	1.933079172	2922.815709	0.065013998
0.08	1678	1.984082301	3329.290101	0.059565981
0.15	1846	2.031980884	3751.036712	0.064810634
0.49	2048	2.08542311	4270.946529	0.06038247
0.65	2256	2.136468371	4819.872644	0.072010249
0.87	2532	2.199012101	5567.898639	0.026572931
1.08	2642	2.222516005	5871.887285	0.025035209
1.31	2750	2.244888976	6173.444685	0.026034912
1.4	2867	2.268394664	6503.487503	0.016562869
1.54	2944	2.28347439	6722.548605	0.021284319
1.84	3046	2.303001223	7014.941725	0.024342386
1.99	3167	2.325539442	7364.983412	0.01443472
2.25	3241	2.339006623	7580.720466	0.007475797
2.38	3280	2.346011598	7694.918041	0.015988975
2.51	3365	2.361065096	7944.984047	0.011957116
2.76	3430	2.372385297	8137.281569	0.042074449
2.84	3669	2.412673876	8852.100451	0.033644811
3.22	3872	2.445375355	9468.493375	0.061949832
3.88	4276	2.506808265	10719.11214	-1

SP-850				
Time (sec)	Vp (m/sec)	Density (g/cc)	Acoustic Impedence "Z"	Reflection Coefficient "RC"
0.02	1512	1.933079172	2922.815709	0.025508212
0.08	1575	1.95290822	3075.830446	0.034717199
0.15	1665	1.980228256	3297.080047	0.128681694
0.56	2048	2.08542311	4270.946529	0.056505133
0.67	2242	2.133146073	4782.513495	0.052844299
0.95	2440	2.178758781	5316.171425	0.034371371
1.08	2578	2.208932383	5694.627684	0.032809736
1.31	2717	2.238123789	6080.982336	0.010040039
1.49	2761	2.247130506	6204.327326	0.018948711
1.66	2846	2.264229361	6443.996762	0.023908406
1.95	2957	2.285991046	6759.675523	0.016888496
2.14	3038	2.301487583	6991.919279	0.036735262
2.27	3222	2.33557102	7525.209827	0.020790925
2.55	3331	2.355078306	7844.765839	0.025005478
2.77	3467	2.378757411	8247.151942	0.049998833
3.09	3756	2.42685087	9115.251867	0.043514454
3.3	4027	2.46948903	9944.632323	0.046317575
3.98	4337	2.515701156	10910.59591	-1

1.7 Determination of reflection coefficients for **SP 800 & 850**

SP-900				
Time (sec)	Vp (m/sec)	Density (g/cc)	Acoustic Impedence"Z"	Reflection Coefficient"RC"
0.03	1572	1.951977598	3068.508785	0.068716635
0.15	1755	2.006462161	3521.341093	0.09710469
0.54	2051	2.086186395	4278.768297	0.0561487
0.65	**2244**	2.133621638	4787.846955	0.020544653
0.78	2319	2.151230175	4988.702775	0.055357738
1.06	2534	2.199446216	5573.396712	0.024659709
1.22	2636	2.221253092	5855.22315	0.023723742
1.37	2738	2.242435989	6139.789737	0.02351573
1.54	2843	2.263632438	6435.507021	0.047161206
1.97	3066	2.30677232	7072.563933	0.015898729
2.07	3145	2.321490209	7301.086706	0.021483185
2.27	3255	2.341528467	7621.67516	0.039955167
2.55	3470	2.379271829	8256.073247	0.031939363
2.75	3652	2.409874277	8800.86086	0.033311128
3.13	3852	2.442211452	9407.398514	0.043827566
3.7	4132	2.48543135	10269.80234	0.018184349
3.98	4254	2.503577646	10650.21931	-1

SP-950				
Time (sec)	Vp (m/sec)	Density (g/cc)	Acoustic Impedence"Z"	Reflection Coefficient"RC"
0.02	1512	1.933079172	2922.815709	0.065013998
0.08	1678	1.984082301	3329.290101	0.059565981
0.15	1846	2.031980884	3751.036712	0.064810634
0.49	2048	2.08542311	4270.946529	0.06038247
0.65	2256	2.136468371	4819.872644	0.072010249
0.87	2532	2.199012101	5567.898639	0.026572931
1.08	2642	2.222516005	5871.887285	0.027075936
1.31	2759	2.246723454	6198.710009	0.023994076
1.4	2867	2.268394664	6503.487503	0.016562869
1.54	2944	2.28347439	6722.548605	0.021284319
1.84	3046	2.303001223	7014.941725	0.024342386
1.99	3167	2.325539442	7364.983412	0.01443472
2.25	3241	2.339006623	7580.720466	0.007475797
2.38	3280	2.346011598	7694.918041	0.019691507
2.51	3385	2.364565573	8004.054463	0.017297267
2.76	3480	2.380984153	8285.824851	0.031167562
2.84	3658	2.410863485	8818.938627	0.035519189
3.22	3872	2.445375355	9468.493375	0.061949832
3.88	4276	2.506808265	10719.11214	-1

1.8 Determination of reflection coefficients for **SP 900 & 950**

SP-1000				
Time (sec)	Vp (m/sec)	Density (g/cc)	Acoustic Impedence"Z"	Reflection Coefficient"RC"
0.02	1510	1.932439609	2917.98381	0.015128796
0.08	1547	1.944170156	3007.631232	0.044409682
0.14	1661	1.979037857	3287.181881	0.132554427
0.5	2056	2.087456679	4291.810933	0.058230394
0.65	2257	2.136705085	4822.543377	0.049453559
0.87	2443	2.179428173	5324.343026	0.029473346
1.08	2561	2.205281775	5647.726627	0.038316486
1.47	2723	2.23935839	6097.772895	0.029139785
1.84	2853	2.265620349	6463.814856	0.027003809
2.15	2979	2.290231162	6822.598632	0.034671889
2.39	3149	2.32222801	7312.696002	0.039025321
2.56	3352	2.35878141	7906.635286	0.033739946
2.72	3538	2.390843511	8458.804342	0.036188903
3.06	3749	2.425719358	9094.021871	0.045452032
3.55	4032	2.470255214	9960.069024	0.036705666
3.98	4276	2.506808265	10719.11214	-1

1.9 Determination of reflection coefficients for **SP 1000**

HAKEEM DAHO_01

Formation	Depth(m)
FF ALLUVIUM	0000.000
FF LAKI	0613.000
FF RANIKOT	1163.000
FF KHADRO	1554.000
FF PARH	1644.000
FF UPPER GORU	1911.000
FF LOWER GORU	2292.000
FF UPPER SAND	2292.000
FF BASAL SAND	2955.000
FF TALHAR SHALE	2982.000
FF MASSIVE SANDS	3061.000

HAKEEM DAHO_02

FF ALLUVIUM	0000.000
FF LAKI	0618.000
FF RANIKOT	1169.000
FF KHADRO	1574.000
FF PARH	1656.000
FF UPPER GORU	1934.000
FF LOWER GORU	2275.000
FF UPPER SHALE	2275.000
FF BASAL SAND	2932.000
FF TALHAR SHALE	2953.000
FF MASSIVE SANDS	3042.000

CHAK63_01

FF ALLUVIUM	0000.000
FF LAKI	0618.000
FF RANIKOT	1178.000
FF KHADRO	1508.000
FF PARH	1579.000
FF UPPER GORU	1785.000
FF LOWER GORU	1942.000

CHAK63_03

FF ALLUVIUM	0000.000
FF LAKI	0614.000
FF RANIKOT	1176.000
FF PARH	1615.000
FF UPPER GORU	1846.000
FF LOWER GORU	2005.000
FF UPPER SHALE	2005.000
FF BASAL SAND	2836.000
FF TALHAR SHALE	2860.000
FF MASSIVE SANDS	2937.000

CHAK63_04

FF ALLUVIUM	0000.000
FF LAKI	0603.000
FF RANIKOT	1180.000
FF KHADRO	1600.000
FF PARH	1674.000
FF UPPER GORU	1901.000

```
FF LOWER GORU                              1974.000
FF UPPER SHALE                             1974.000
FF BASAL SAND                              2823.000
FF TALHAR SHALE                            2845.000
FF MASSIVE SANDS                           2932.000
```

CHAK63 SOUTH EAST

```
FF ALLUVIUM                                0000.000
FF LAKI                                     0626.000
FF RANIKOT                                  1165.000
FF KHADRO                                   1541.000
FF PARH                                     1607.000
FF UPPER GORU                               1776.000
FF LOWER GORU                               2051.000
FF UPPER SAND-SHALE-MARL SEQUENCE           2051.000
FF BASAL SAND                               2847.000
FF TALHAR SHALE                             2863.000
FF MASSIVE SANDS                            2947.000
```

CHAK66_01

```
FF ALLUVIUM                                0000.000
FF LAKI                                     0612.000
FF RANIKOT                                  1161.000
FF PARH                                     1631.000
FF UPPER GORU                               1773.000
FF LOWER GORU                               2023.000
FF BASAL SAND                              2842.000
FF TALAR                                    2866.000
```

CHAK7A_1

```
FF ALLUVIUM                                0000.000
FF LAKI                                     0604.000
FF RANIKOT                                  1145.000
FF PARH                                     1642.000
FF UPPER GORU                               1741.000
FF LOWER GORU                               2102.000
FF UPPER SHALE                             2102.000
FF BASAL SAND                              2817.000
FF TALHAR SHALE                            2845.000
FF MASSIVE SANDS                           2915.000
```

1.10 Sinjhoro Wells Data

REFERENCES

References

- Ahmad Naveed "Fundamentals of Seismic Data Interpretation" p-2.
- Al-Sadi H, N, 1980.seismic "Exploration Technique and Processing", Birkhauser Verlag Bostan.
- Badley, M. E., (1985), "Practical Seismic Interpretation", D. Riedel Publishing Company. International Human Resources Development Cooperation, Dordrecht, Holland.
- Dobrin M.B & Savit C.H. (1976), "Introduction to Geophysical Prospecting",
- Dobrin M.B & Savit C.H. (1988, 1998), "Introduction to Geophysical Prospecting", 4th Edition, McGraw-Hill Book Company, London.
- Fatmi (1968),"The Paleontology and Stratigraphy of Mesozoic Rocks of Western Kohat, Kala Chitta, Hazara and Trans-Indus Salt Ranges,West Pakistan".
- Fatmi (1972),"Stratigraphy of Juriassic and Lower Cretaceous Rocks and Juriassic ammonites from Northern areas of West Pakistan"; British Mus.Nat.Hist., (Geol).
- Ibrahim Shah, Gelogical Survey of Pakistan: 1977 "Strarigraphy of Pakistan" Volume 12.
- Iqbal B Kadri, 1995 "Petroleum Geology of Pakistan".
- Kazmi, A.H. & Jan, M.Q. (1997). "Geology & Tectonics of Pakistan", Graphic Publishers, Karachi, Pakistan 560p.
- Keary, P & Brooks M.2002, "An Introduction to Geophysical Exploration", Blackwell Scientific Publications, Oxford
- N.A Zaigham: 2000 "Prospect of Hyderocarbons associated with fossil rift structures of Southern Indus Basin".
- Orient Petroleum International Report, January 01, 2010.
- Pakistan Petroleum Information Service: Report"Lower Indus Platform Basin" (ppisonline.com/JOP2010/data/technical..../lower Indus Platform.pdf).